Tree Physiology, 2025, **45**, tpaf119
https://doi.org/10.1093/treephys/tpaf119
Advance access publication date 25 September 2025
Research paper

Increasing nitrogen availability increases water-use efficiency and decreases nitrogen-use efficiency in *Acer saccharum*

Evan A. Perkowski[1,*], David W. Frey[2], Christine L. Goodale[2] and Nicholas G. Smith[1]

[1]Department of Biological Sciences, Texas Tech University, 2901 Main St., Lubbock, TX 79409, USA
[2]Department of Ecology and Evolutionary Biology, 215 Tower Rd, Corson Hall, Cornell University, Ithaca, NY 14853, USA

*Corresponding author (evan.a.perkowski@ttu.edu)

Handling Editor: Rossella Guerrieri

Photosynthesis links terrestrial carbon, water and nutrient cycles. Photosynthetic least-cost theory suggests that plants optimize photosynthesis at the lowest summed investments in nutrient and water use. The theory predicts that increasing nutrient availability should increase nutrient allocation toward photosynthetic enzymes and reduce stomatal conductance, allowing similar photosynthetic rates achieved at a lower ratio of leaf intercellular to atmospheric CO_2 concentration (χ) and reduced water loss. The theory suggests similar responses to increasing soil pH in acidic soils due to common correlations between soil pH and nutrient availability. However, empirical tests of the theory outside of environmental gradients are rare. To test this theory experimentally, we measured photosynthetic traits in mature *Acer saccharum* Marshall trees growing in a 9-year, nitrogen-by-pH manipulation in the northeastern USA. Increasing soil nitrogen availability did not affect net photosynthesis (A_{net}) or stomatal conductance (g_s) rates, but was associated with increased area-based leaf nitrogen content (N_{area}), increased photosynthetic capacity (V_{cmax}, J_{max}) and decreased χ (i.e, increased water-use efficiency). These patterns strengthened the tradeoff between nitrogen and water use, indicated by steeper slopes of N_{area}–χ and V_{cmax}–χ with increasing soil nitrogen availability. When examined across all plots, soil pH had no effect on any traits. However, in plots without nitrogen additions, increasing soil pH increased the slopes of N_{area}–χ and V_{cmax}–χ, though did not modify χ. Supporting the theory, *A. saccharum* maintained A_{net} across the soil nitrogen availability gradient by trading less efficient nitrogen use for more efficient water use. Additionally, the effects of soil pH on nitrogen–water use tradeoffs appear to occur through indirect pH effects on soil nitrogen availability. These results indicate that elevated nitrogen deposition could stimulate photosynthesis less than commonly expected and instead reduce water losses, and conversely, that reductions in photosynthesis expected from increasing nitrogen limitation in some regions could be lessened if accompanied by increased transpiration.

Keywords: least-cost theory, nutrient addition, nutrient allocation, photosynthetic capacity, plant functional ecology, soil pH.

Introduction

Photosynthesis represents the largest carbon flux between the atmosphere and land surface (IPCC 2021) and plays a central role in biogeochemical cycling at multiple spatiotemporal scales (Vitousek and Howarth 1991, LeBauer and Treseder 2008, Wieder et al. 2015). Therefore, carbon and energy fluxes simulated by terrestrial biosphere models are sensitive to the formulation of photosynthetic processes (Bonan et al. 2011, Ziehn et al. 2011, Booth et al. 2012, Smith et al. 2016, 2017) and must be represented using robust, empirically tested processes (Prentice et al. 2015, Wieder et al. 2019). Current formulations of photosynthesis vary across terrestrial biosphere models (Smith and Dukes 2013, Rogers et al. 2017), which causes variation in modeled ecosystem processes (Knorr 2000, Knorr and Heimann 2001, Bonan et al. 2011, Friedlingstein et al. 2014) and casts uncertainty on the ability of these models to predict terrestrial ecosystem responses and feedbacks to global change accurately (Zaehle et al. 2005, Schaefer et al. 2012, Davies-Barnard et al. 2020).

Terrestrial biosphere models commonly represent C_3 photosynthesis through the Farquhar et al. (1980) biochemical model (Smith and Dukes 2013, Rogers 2014, Rogers et al. 2017, Stocker et al. 2025). This well-tested photosynthesis model estimates leaf-level carbon assimilation, or photosynthetic capacity, as a function of the maximum rate of Ribulose-1,5-bisphosphate carboxylase-oxygenase (Rubisco) carboxylation (V_{cmax}) and the maximum rate of electron transport for Ribulose-1,5-bisphosphate (RuBP) regeneration (J_{max}; Farquhar et al. 1980). Many terrestrial biosphere models predict these model inputs based on plant functional group-specific relationships between area-based leaf nitrogen content (N_{area}) and V_{cmax} (Smith and Dukes 2013, Rogers 2014, Rogers et al. 2017, Stocker et al. 2025) under the tenet that a large fraction of leaf nutrients, and nitrogen in particular, is partitioned toward building and maintaining enzymes that support photosynthetic capacity, such as Rubisco (Brix 1971, Gulmon and Chu 1981, Evans 1989, Kattge et al. 2009, Walker et al. 2014). Terrestrial biosphere models predict leaf nutrient content from soil nutrient availability based on ample evidence showing that increasing soil nutrient availability generally increases leaf nutrients (Firn et al. 2019, Li et al. 2020, Liang et al. 2020, Stocker et al. 2025, Cheaib et al. 2025*b*) which, in the case of nitrogen, often corresponds with an increase in photosynthetic capacity (Walker et al. 2014, Waring et al. 2023, Perkowski et al. 2025).

Recent work calls the generality of relationships between soil nutrient availability, leaf nutrient content and

Received: December 6, 2024. **Accepted:** September 15, 2025

photosynthetic capacity into question, suggesting that leaf nutrients and photosynthetic capacity are better predicted as an integrated product of aboveground climate, leaf traits and soil properties, rather than soil nutrient availability alone (Dong et al. 2017, 2020, 2022, Firn et al. 2019, Smith et al. 2019, Peng et al. 2021, Stocker et al. 2025, Cheaib et al. 2025*b*). It has been reasoned that this result is because plants allocate added nutrients to growth and storage rather than alterations in leaf chemistry (Smith et al. 2019, Waring et al. 2023, Perkowski et al. 2025), perhaps as a result of nutrient limitation of primary productivity (LeBauer and Treseder 2008, Fay et al. 2015). Additionally, recent work suggests that relationships between leaf nutrient content and photosynthesis vary across environments and that the proportion of leaf nutrient content allocated to photosynthesis varies over space and time with plant acclimation and adaptation responses to light availability, vapor pressure deficit, soil pH, soil nutrient availability and environmental factors that influence leaf mass per unit leaf area (Pons and Pearcy 1994, Niinemets and Tenhunen 1997, Evans and Poorter 2001, Hikosaka and Shigeno 2009, Ghimire et al. 2017, Onoda et al. 2017, Luo et al. 2021, Waring et al. 2023, Perkowski et al. 2025). The use of parameterized relationships between leaf nutrients and V_{cmax} to predict photosynthetic capacity, as commonly used in terrestrial biosphere models (Rogers 2014), is not capable of detecting such responses.

Photosynthetic least-cost theory provides an alternative framework for understanding relationships between soil nutrient availability, leaf nutrient content and photosynthetic capacity (Harrison et al. 2021). Using a two-input microeconomics approach (Wright et al. 2003), the theory posits that plants acclimate to a given environment by optimizing leaf photosynthesis rates at the lowest summed cost of using nutrients and water (Prentice et al. 2014, Wang et al. 2017, Smith et al. 2019, Paillassa et al. 2020). Across resource availability gradients, the theory predicts that optimal photosynthetic rates can be achieved by trading less efficient use of a resource that is less costly to acquire (or more abundant) for more efficient use of a resource more costly to acquire (or less abundant). For example, an increase in soil nutrient availability should reduce the cost of acquiring and using nutrients (Bae et al. 2015, Eastman et al. 2021, Perkowski et al. 2021, 2024, Cheaib et al. 2025*a*), which could increase leaf nutrient investments in photosynthetic proteins to allow similar photosynthetic rates to be achieved with higher nutrient use (lower nutrient-use efficiency) and lower water use (greater water-use efficiency; indexed here as the ratio of intercellular CO_2 to atmospheric CO_2, or leaf C_i:C_a).

Photosynthetic least-cost theory suggests similar tradeoffs in response to soil pH because increasing soil pH is often associated with greater soil nutrient availability (Paillassa et al. 2020). Indeed, soil pH can alter ecosystem nitrogen mineralization rates and nitrogen availability (e.g. through changes in soil microbial community biomass; Li et al. 2019), and has been asserted to be a dominant control of phosphorus forms in topsoils (Hou et al. 2018). If soil pH affects soil nutrient availability, then changes in soil pH should lead to nutrient–water use tradeoffs predicted by photosynthetic least-cost theory. For example, in acidic soils, increasing soil pH should reduce the cost of acquiring nutrients due to an increase in plant-available nutrient concentration (Paillassa et al. 2020, Dong et al. 2022), allowing similar photosynthetic rates to be achieved with higher nutrient use and lower water use. Opposite patterns may be expected in alkaline soils, where increasing soil pH may increase the cost of acquiring nutrients due to a decrease in plant-available nutrient concentrations (Truog 1947), allowing similar photosynthetic rates achieved with lower nutrient use and higher water use. Although the effects of soil pH on patterns expected from photosynthetic least-cost theory have not been tested experimentally, previous work using environmental gradients has demonstrated effects of soil pH on nutrient–water use tradeoffs that are supportive of the theory (Paillassa et al. 2020).

Nitrogen–water use tradeoffs expected from photosynthetic least-cost theory have recently received empirical support both in global environmental gradient (Paillassa et al. 2020, Querejeta et al. 2022, Fan et al. 2023, Westerband et al. 2023) and local manipulative invasion (Bialic-Murphy et al. 2021) studies, but have yet to be directly assessed through a nutrient addition experiment. Furthermore, only environmental gradient studies testing the theory have considered soil pH in their analyses. Quantifying plant ecophysiological responses to soil nitrogen and soil pH is important for understanding ecosystem biogeochemical cycle dynamics both in regions undergoing acidification from high rates of nitrogen and sulfate deposition (e.g. east Asia) and in regions recovering from historically high deposition rates (e.g. the northeastern USA and much of central and northern Europe, Vet et al. 2014).

Recent work in a soil nitrogen-by-pH manipulation experiment in mixed hardwood forests suggests that soil nitrogen availability, rather than soil acidification, is the stronger driver of changes in the belowground plant and soil processes that contribute to soil respiration (Frey et al. 2025). This factorial field experiment also provided an opportunity to examine the roles of soil nitrogen availability and soil acidification in affecting a range of important photosynthetic processes (including net photosynthesis, stomatal conductance, and photosynthetic capacity), and to assess whether aboveground and belowground biogeochemical processes respond similarly to manipulations of soil nitrogen and acidity. Thus, the experiment described herein provides a valuable opportunity to disentangle these two soil influences of acid deposition, while also evaluating whether photosynthetic responses to experimentally altered soil resource availability follow predictions from photosynthetic least-cost theory.

In this study, leaf responses to soil nitrogen availability were assessed for sugar maple (*Acer saccharum* Marshall) trees growing in mature temperate forests in the northeastern USA. *Acer saccharum* is an abundant, late-successional tree species in northern hardwood forests that shapes ecosystem biogeochemical cycles through nutrient-rich, fast-decomposing leaf litter, while also supporting regional economies through its use in timber and maple syrup production (Lovett and Mitchell 2004). Soil nitrogen availability and pH were modified through a long-term nitrogen-by-pH field manipulation experiment. Two different soil nitrogen treatments were applied to increase nitrogen availability with opposing effects on soil pH. An additional nitrogen-free acidifying treatment was applied to decrease soil pH. We hypothesized that increased soil nitrogen availability would enable plants to increase nutrient uptake and create more photosynthetic enzymes per leaf, allowing similar photosynthetic rates achieved with lower leaf C_i:C_a and increased leaf nitrogen content allocated to photosynthetic leaf tissue. A reduction

in leaf C_i:C_a with increasing soil nitrogen availability in our study would be reflective of a reduction in stomatal conductance that allows plants to maintain photosynthetic rates under increasing water stress by enhancing water-use efficiency (Paillassa et al. 2020, Querejeta et al. 2022, Westerband et al. 2023). It would likely not reflect a change in CO_2 drawdown because light availability is expected to set maximum rates of photosynthetic carbon assimilation (Wright et al. 2003) and full-sun leaves were used for all measurements. We expected that leaf responses to increased soil nitrogen availability would be driven by a reduction in the cost of acquiring nitrogen, which would cause trees to sacrifice efficient nitrogen use to enable more efficient use of other limiting resources (i.e. water). We hypothesized opposite leaf responses to decreasing soil pH in the absence of nitrogen addition.

Materials and methods

Study site description

This study was conducted in summer 2019 at three mature forest stands located within a 20-km radius of Ithaca, NY, USA (42.444° N, 76.502° W), dominated by late-successional mixed deciduous tree species. Stands contained abundant sugar maple (*A. saccharum* Marshall), accounting for 43% of the total aboveground biomass across the three stands, with less abundant American beech (*Fagus grandifolia* Ehrh., 15%), white ash (*Fraxinus americana* L., 17%), red maple (*Acer rubrum* L.; 9%) and red oak (*Quercus rubra* L.; 10%). Soils at each site were broadly classified as channery silt loam Inceptisols using the USDA NRCS Web Soil Survey data product (Soil Survey Staff 2022). Between 1991 and 2020, the closest weather station located near the Cornell University campus (42.449° N, 76.449° W and part of the NOAA NCEI Global Historical Climatology Network; Menne et al. 2012), received an average of 972 mm of precipitation per year and had an annual average temperature of 7.9 °C. Measurements from a nearby Clean Air Status and Trends Network monitoring site show large declines in atmospheric deposition of nitrogen and sulfur between 2000 and 2021: nitrogen deposition (wet + dry, including NH_3) decreased from 13.4 to 8.9 kg N ha^{-1} $year^{-1}$, while sulfur deposition decreased from 13.0 to 1.7 kg S ha^{-1} $year^{-1}$ (CASTNET 2024). These trends are consistent with regional declines in nitrogen and sulfur emissions in response to the Clean Air Act and its 1990 Amendments (Driscoll et al. 2024).

Experimental design

At each of the three mature stands, four 40 m × 40 m plots were established in 2009 (12 plots total across stands), and all trees with greater than or equal to 9.5 cm diameter at breast height were inventoried and tagged. The plots were set up as a nitrogen-by-pH field manipulation experiment, with four treatments at each site applied since 2011 to the core plot and an additional 10 m buffer along plot perimeters (60 m × 60 m total). Two nitrogen treatments were applied, both at 50 kg N ha^{-1} $year^{-1}$, as either sodium nitrate ($NaNO_3$) to raise soil pH, or ammonium sulfate ($(NH_4)_2SO_4$) to acidify (S application rate of 54 kg S ha^{-1} $year^{-1}$); an elemental sulfur treatment was selected to acidify soils without nitrogen addition, applied at the same rate of sulfur addition as in the ammonium sulfate treatment. Control plots received no additions. Amendment rates are similar to rates of nitrogen and sulfur deposition to parts of Europe during the 1980s and 1990s and in contemporary eastern China (Dise and Wright 1995, Kolář et al. 2015, Zhou et al. 2023).

All amendments were added in pelletized form using hand-held fertilizer spreaders to both the main plots and buffers. Amendments were divided into three equal doses distributed across the growing season from 2011 to 2017 and added as a single dose at the beginning of the growing season from 2018 onward. During 2019, plots were fertilized during the week of 20 May. Previous work in this experiment in these and in three younger adjacent stands has shown that nitrogen addition decreases annual soil respiration fluxes through suppression of both root-associated respiration (∼2/3) and heterotropic respiration (∼1/3), with no net effect of soil acidification (Frey et al. 2025).

Leaf gas exchange and trait measurements

We sampled one canopy leaf each from 6 to 10 dominant broadleaf trees per plot between 25 June and 12 July 2019 for gas exchange measurements (Table S1 available as Supplementary Data at *Tree Physiology* Online). Trees were selected to reflect dominant species composition in each plot. Gas exchange measurements were conducted on all target leaves ($n = 98$; Table S1 available as Supplementary Data at *Tree Physiology* Online) and are included in Supplemental Information. Only one species, *A. saccharum*, occurred on all twelve plots and in sufficient abundance ($n = 2$–7 samples per plot, 47 total; Table S1 available as Supplementary Data at *Tree Physiology* Online) to confidently test our hypotheses, and so it forms the focus of this study.

Gas exchange measurements were collected during the growing season several weeks after full leaf expansion to minimize any effect of seasonal phenology on plant physiology. We sought to collect leaves from the upper canopy to reduce differential shading effects on leaf physiology. Leaves were accessed by pulling down small branches using an arborist's slingshot and weighted beanbag attached to a throwline. Branches were immediately recut under deionized water and remained submerged to reduce stomatal closure and avoid xylem embolism (as in Smith and Dukes 2018) until gas exchange data were collected. Randomly selected leaves with little to no visible external damage were attached to a Li-COR LI-6800 (Li-COR Bioscience, Lincoln, NE, USA) portable photosynthesis machine to measure net photosynthesis (A_{net}; μmol m^{-2} s^{-1}), stomatal conductance (g_s; mol m^{-2} s^{-1}) and intercellular CO_2 concentration (C_i; μmol mol^{-1}) at different atmospheric CO_2 (C_a; μmol mol^{-1}) concentrations (i.e. an A_{net}/C_i curve) under saturating light conditions (2000 μmol m^{-2} s^{-1}) after leaves stabilized in the cuvette. Reference CO_2 concentrations (C_a; μmol mol^{-1}) followed the sequence: 400, 300, 200, 100, 50, 400, 400, 600, 800, 1000, 1200, 1500 and 2000 μmol mol^{-1}. A_{net}/C_i curves were not collected if stomatal conductance rates at the starting CO_2 concentration were below 0.01 mol m^{-2} s^{-1}, as these values were considered indicative of stress associated with branch severance (Bahar et al. 2017). Instead, a new full-sun branch was brought down from the same tree and a new leaf was stabilized in the LI-6800 cuvette. In all cases, this approach yielded stomatal conductance rates above 0.01 mol m^{-2} s^{-1}. Leaf temperatures were not controlled in the cuvette and ranged from 21.8 °C to 31.7 °C (mean ± SD: 27.2 ± 2.2 °C). However, a linear and second order log-polynomial nonlinear

regression suggested no effect of cuvette leaf temperature on stomatal conductance or net photosynthesis when measured at 400 μmol mol^{-1} CO_2 (Tables S2 and S3, and Figure S1 available as Supplementary Data at *Tree Physiology* Online). All A_{net}/C_i curves were generated within one hour of branch severance.

Leaf morphological and chemical traits were collected on the same leaf used to generate each A_{net}/C_i curve. Images of each leaf were collected using a flat-bed scanner to determine fresh leaf area using the 'LeafArea' R package (Katabuchi 2015), which automates leaf area calculations using ImageJ software (Schneider et al. 2012). Each leaf was dried at 65 °C for at least 48 h, weighed and ground using a Retsch MM200 ball mill grinder (Verder Scientific, Inc., Newtown, PA, USA) until homogenized. Leaf mass per area (M_{area}; g_{dry_mass} m_{leaf}^{-2}) was calculated as the ratio of dry leaf biomass to fresh leaf area. Using a subsample of ground and homogenized leaf biomass, leaf nitrogen content (N_{mass}; gN $g_{dry\_mass}^{-1}$) and leaf $\delta^{13}C$ (‰, relative to Vienna Pee Dee Belemnite international reference standard) were measured at the Cornell University Stable Isotope Lab with an elemental analyzer (NC 2500, CE Instruments, Wigan, UK) interfaced to an isotope ratio mass spectrometer (Delta V Isotope Ratio Mass Spectrometer, ThermoFisher Scientific, Waltham, MA, USA). Leaf nitrogen content per unit leaf area (N_{area}; gN m_{leaf}^{-2}) was calculated by multiplying N_{mass} and M_{area}.

Leaf $\delta^{13}C$ values were used to estimate χ (unitless), which is an isotope-derived estimate of the ratio between the leaf intercellular CO_2 concentration to the atmospheric CO_2 concentration (or leaf C_i:C_a). This trait corresponds with an increase in stomatal conductance and water loss per unit CO_2 gain, and can be interpreted as an inverse proxy of water-use efficiency. While intercellular and atmospheric CO_2 concentrations were directly measured during each A_{net}/C_i curve, deriving χ from $\delta^{13}C$ provides an integrative estimate of the leaf C_i:C_a over an individual leaf's lifespan. We derived χ following the approach of Farquhar et al. (1989):

$$\chi = \frac{\Delta^{13}C - a}{b - a} \tag{1}$$

where $\Delta^{13}C$ represents the relative difference between leaf $\delta^{13}C$ (‰) and air $\delta^{13}C$ (‰), a represents the fractionation between ^{12}C and ^{13}C due to diffusion in air, assumed to be 4.4‰, and b represents the fractionation caused by Rubisco carboxylation, assumed to be 27‰ (Farquhar et al. 1989). $\Delta^{13}C$ was calculated as:

$$\Delta^{13}C = \frac{\delta^{13}C_{air} - \delta^{13}C_{leaf}}{1 + \left(\frac{\delta^{13}C_{leaf}}{1000}\right)} \tag{2}$$

where $\delta^{13}C_{air}$ was assumed to be −8‰ (Keeling et al. 1979, Farquhar et al. 1989).

A_{net}/C_i curve-fitting and parameter estimation

A_{net}/C_i curves were fit for each individual tree using the 'fitaci' function in the 'plantecophys' R package (Duursma 2015). This function estimates the maximum rate of Rubisco carboxylation (V_{cmax}; μmol m^{-2} s^{-1}) and maximum rate of electron transport for RuBP regeneration (J_{max}; μmol m^{-2} s^{-1}) based on the Farquhar et al. (1980) biochemical model of C_3 photosynthesis. For each curve fit, triose phosphate utilization (TPU) was included as an additional rate-limiting step to avoid underestimating J_{max} (Gregory et al. 2021). Curves were visually examined to confirm the likely presence of TPU limitation. Curve fits assumed that mesophyll conductance was non-limiting and were fit using intercellular CO_2 concentration. This approach may risk underestimating V_{cmax} due to mesophyll resistance slowing the rate of Rubisco carboxylation (Evans 2021). We determined Michaelis–Menten coefficients for Rubisco affinity to CO_2 (K_c; μmol mol^{-1}) and O_2 (K_o; mmol mol^{-1}), and the CO_2 compensation point (Γ^*; μmol mol^{-1}) using leaf temperature and equations derived in Bernacchi et al. (2001). Specifically, K_c and K_o were calculated as:

$$K_c = 404.9 * \exp\left(\frac{79430(T_k - 298)}{298RT_k}\right) \tag{3a}$$

and

$$K_o = 278.4 * \exp\left(\frac{36380(T_k - 298)}{298RT_k}\right) \tag{3b}$$

while Γ^* was calculated as:

$$\Gamma^* = 42.75 * \exp\left(\frac{37830(T_k - 298)}{298RT_k}\right) \tag{3c}$$

In all three equations, T_k is the leaf temperature (in Kelvin) during each A_{net}/C_i curve and R is the universal gas constant (8.314 J mol^{-1} K^{-1}).

V_{cmax} and J_{max} were standardized to 25 °C using a modified Arrhenius equation as done in Kattge and Knorr (2007):

$$f(T) = e^{\left[\frac{H_a(T_{leaf} - T_{reference})}{RT_{leaf}298.15}\right]} \frac{1 + e^{\left(\frac{T_{reference}(\Delta S) - H_d}{RT_{reference}}\right)}}{1 + e^{\left(\frac{T_{leaf}(\Delta S) - H_d}{RT_{leaf}}\right)}} \tag{4}$$

and

$$k_{25} = \frac{k_{Tleaf}}{f(T)} \tag{5}$$

k_{25} represents the standardized V_{cmax} or J_{max} rate at 25 °C, k_{Tleaf} represents V_{cmax} or J_{max} at the average leaf temperature measured inside the cuvette during the A_{net}/C_i curve. H_a is the activation energy of V_{cmax} (71,513 J mol^{-1}; Kattge and Knorr 2007) or J_{max} (49,884 J mol^{-1}; Kattge and Knorr 2007). H_d represents the deactivation energy of both V_{cmax} and J_{max} (200,000 J mol^{-1}; Medlyn et al. 2002), and R represents the universal gas constant (8.314 J mol^{-1} K^{-1}). $T_{reference}$ represents the standardized temperature of 298.15 K (25 °C) and T_{leaf} represents the mean leaf temperature (in K) during each A_{net}/C_i curve. ΔS is an entropy term that Kattge and Knorr (2007) derived as a linear relationship with average growing season temperature (T_g; °C), where:

$$\Delta S_{vcmax} = -1.07T_g + 668.39 \tag{6a}$$

and:

$$\Delta S_{jmax} = -0.75T_g + 659.70 \tag{6b}$$

T_g was estimated using the mean daily air temperature of the 30 days leading up to the day of each sample collection using the same weather station reported in the site description. Given that this weather station is positioned ~200 m lower elevation (293 m.a.s.l.) than the experimental sites (mean ± SD: 510.1 ± 46.7 m.a.s.l.), it should report slightly higher temperatures (~1–1.5 °C). These climate data therefore overestimate ΔS_{vcmax} and ΔS_{jmax} and slightly underestimate V_{cmax25} and J_{max25}. However, comparisons across sites were not expected to be influenced by this, as the three sites were positioned at similar elevations.

Finally, we calculated the ratio of J_{max25} to V_{cmax25} (J_{max25}:V_{cmax25}; unitless).

Tradeoffs between nitrogen and water use

Photosynthetic nitrogen-use efficiency (*PNUE*; μmol CO_2 mol^{-1} N s^{-1}) was calculated by dividing A_{net} by N_{area}, first converting N_{area} to mol N m_{leaf}^{-2} using the molar mass of nitrogen (14 g mol^{-1}). We used χ as an indicator of water-use efficiency, where high χ values are indicative of high stomatal conductance and low water-use efficiency. Tradeoffs between nitrogen and water use were determined by calculating the slope relationship between N_{area} and χ (N_{area}–χ; gN m_{leaf}^{-2}), between V_{cmax25} and χ (V_{cmax25}–χ; μmol m^{-2} s^{-1}), and between *PNUE* and χ (*PNUE*–χ; μmol CO_2 mol^{-1} N s^{-1}) across the soil nitrogen availability and soil pH gradient. This approach is similar to calculations used in previous studies, where nitrogen–water use tradeoffs were measured as the ratio of N_{area} or V_{cmax25} to stomatal conductance (Paillassa et al. 2020, Bialic-Murphy et al. 2021). Here, these relationships were quantified using χ because stomatal conductance changes rapidly with environmental conditions and may have been altered by recent tree branch severance or placement in the cuvette. We also quantified slope relationships using χ because this trait is integrated across the lifespan of a leaf and therefore should acclimate over a more similar timescale with N_{area} and V_{cmax25} than an instantaneous stomatal conductance rate.

Soil nitrogen availability and soil pH

To characterize soil nitrogen availability at the time of leaf gas exchange measurements, we used mixed bed resin bags to quantify mobile ammonium-N and nitrate-N concentrations in each plot. Lycra mesh bags were filled with 5 g of Dowex Marathon MR-3 hydrogen and hydroxide form resin (MilliporeSigma, Burlington, MA, USA) and sealed with a zip tie. Each bag was activated by soaking in 0.5 M HCl for 20 min, then in 2 M NaCl until pH of the saline solution stabilized, as described in Allison et al. (2008). Five resin bags were inserted about 10 cm below the soil surface at each plot on 25 June 2019: one placed near each of the four plot corners, and one placed near the plot center. All resin bags were collected 24 days later on 19 July 2019, and were frozen until extracted.

Each resin bag was rinsed with ultrapure water (MilliQ IQ 7000; Millipore Sigma, Burlington, MA, USA) to remove any surface soil residues prior to anion and cation extraction. Anions and cations were extracted from surface-cleaned resin bags by individually soaking each bag in 100 mL of a 0.1 M HCl/2.0 M NaCl matrix and shaking with an Innova™ 2000 platform shaker (New Brunswick Scientific, Edison, NJ, USA) for 1 h at room temperature (~25 °C). Using a microplate reader (Biotek Synergy H1; Biotek Instruments, Winooski, VT, USA), nitrate-N concentrations were quantified spectrophotometrically at 540 nm with the end product of a single reagent vanadium (III) chloride reaction (Doane and Horwáth 2003), while ammonium-N concentrations were quantified at 650 nm with the end product of a modified phenol-hypochlorite reaction (Weatherburn 1967, Rhine et al. 1998). Both the single reagent vanadium (III) chloride and modified phenol-hypochlorite reactions are well established methodologies for determining nitrate-N and ammonium-N concentrations in resin bag extracts (Arnone 1997, Allison et al. 2008). Negative and positive controls were used throughout each well plate to verify the accuracy and precision of measurements, with each resin bag extract and control assayed in triplicate. Soil nitrogen availability was estimated as the sum of the nitrate-N and ammonium-N concentration in each resin bag, normalized per g of resin and duration in the field (μg N g_{resin}^{-1} day^{-1}), then averaged across all resin bags in a plot for a plot-level mean.

It is unlikely that soil water status influenced ion exchange rates across plots and sites. This conclusion is supported by data from a nearby weather station, which reported 11% greater precipitation during the 12 months leading up to our measurement period (1082 mm) compared with the 1991–2020 annual precipitation normal (972 mm). Furthermore, precipitation during the specific period where resin bags were deployed closely matched the 1991–2020 monthly precipitation normal. Specifically, precipitation in June was 137% of normal expectations (138 mm received compared with 101 mm normally expected), while precipitation in July was 96% of normal expectations (95 mm received compared with 99 mm normally expected).

Soil pH was measured on 0–10 cm mineral soil samples collected immediately prior to fertilization in May 2019. Near each of the four plot corners, three 6 cm diameter soil cores were collected after first removing the forest floor where present. Each set of three cores was placed in a plastic bag, and later composited by hand mixing and sieved to 4 mm. Soil pH was determined for a 1:2 soil:water slurry (10 g field-moist soil to 20 mL DI water) of each sample using an Accumet AB15 pH meter with a flushable junction probe (Fisher Scientific; Hampton, NH, USA), and was estimated at the plot level as the mean soil pH within each plot.

Statistical analyses

Three series of linear mixed-effects models were built to explore effects of soil nitrogen availability, soil pH and area-based leaf nitrogen content on *A. saccharum* leaf physiological traits ($n = 47$). Parallel analyses including all measured species (n = 10–18 per species) are reported in the Supplemental Information (Tables S14–S16, and Figures S6–S8 available as Supplementary Data at *Tree Physiology* Online).

In the first series of linear mixed-effects models, we explored the effect of soil nitrogen availability and soil pH on *A. saccharum* leaf nitrogen content, leaf photosynthesis, resource-use efficiency and nitrogen–water use tradeoffs. Models included soil nitrogen availability and soil pH as continuous fixed effects, and site was designated as a random intercept term. Soil nitrogen availability and soil pH were included as continuous variables in lieu of categorical treatments due to the high degree of heterogeneity of soil nitrogen availability and soil pH within treatments across sites (Table S4 available as Supplementary Data at *Tree Physiology* Online). Interaction terms between fixed effects were not included due to the small number of experimental plots. We built a series

of separate models with this independent variable structure to quantify individualeffects of soil nitrogen availability, soil pH, and species on N_{area}, M_{area}, N_{mass}, A_{net}, V_{cmax25}, J_{max25}, J_{max25}:V_{cmax25}, χ, *PNUE*, the N_{area}–χ slope, the V_{cmax25}–χ slope and the *PNUE*–χ slope. To understand whether these traits were more strongly associated with soil nitrate or soil ammonium availability, parallel analyses that isolate the effects of soil nitrate availability and soil ammonium availability on these traits were quantified using the same independent variable structure described above, replacing soil nitrogen availability with either soil nitrate availability or soil ammonium availability (Tables S6, S8 and S10, and Figures S3–S5 available as Supplementary Data at *Tree Physiology* Online).

Nitrogen addition treatments increased soil nitrogen availability, while the different forms of nitrogen addition had different effects on soil pH, as intended (Figure S2 available as Supplementary Data at *Tree Physiology* Online). To isolate the effect of soil pH on measured leaf traits, we constructed a second series of linear mixed-effects models using only measurements collected from the control and sulfur treatments that acidified the soil without adding nitrogen (Table S5 and Figure S2 available as Supplementary Data at *Tree Physiology* Online). Models included soil pH as a fixed effect and site as a random intercept term and were constructed for each of the response variables (N_{area}, M_{area}, N_{mass}, A_{net}, V_{cmax25}, J_{max25}, J_{max25}:V_{cmax25}, χ, *PNUE*, the N_{area}–χ slope, the V_{cmax25}–χ slope and the *PNUE*–χ slope).

A third series of linear mixed-effects models were built to investigate relationships between area-based leaf nitrogen content and photosynthetic parameters. Statistical models included N_{area} as a fixed effect and site as a random intercept term. We used this independent variable structure to quantify individual effects of leaf nitrogen content on A_{net}, V_{cmax25}, J_{max25}, J_{max25}:V_{cmax25}, χ and the V_{cmax25}–χ slope.

For all linear mixed-effects models, Shapiro–Wilk tests of normality were used to determine whether models satisfied residual normality assumptions. If residual normality assumptions were not met, then models were fit using dependent variables that were natural log transformed. If residual normality assumptions were still not met (Shapiro–Wilk: $P < 0.05$), then models were fit using dependent variables that were square root transformed. Residual normality assumptions were met in the first series of linear mixed-effects models with untransformed response variables for all models, except for A_{net} (square root transformation required) stomatal conductance (natural log transformation required) and *PNUE* (square root transformation required). Residual normality assumptions were met in the second series of models with untransformed response variables for all models except A_{net}, stomatal conductance, *PNUE* and the *PNUE*–χ slope (square root transformation required in all cases). Finally, residual normality assumptions were met in the third series of models with untransformed response variables for all models except for A_{net} (square root transformation required), stomatal conductance (natural log transformation required) and *PNUE* (square root transformation required).

In all models, we used the 'lmer' function in the 'lme4' R package (Bates et al. 2015) to fit each model and the 'Anova' function in the 'car' R package (Fox and Weisberg 2019) to calculate Type II Wald's χ^2 and determine the significance level ($\alpha = 0.05$) of each fixed effect coefficient. We also used the 'emmeans' R package (Lenth 2019) to conduct post-hoc comparisons using Tukey's tests, where degrees of freedom were approximated using the Kenward-Roger approach (Kenward and Roger 1997). All analyses and plots were conducted in R version 4.1.0 (R Core Team 2021). All figure regression lines and associated 95% confidence interval error bars were plotted using predictions generated across the soil nitrogen availability or soil pH gradient using the 'emmeans' R package (Lenth 2019). In addition to linear mixed-effects models, we constructed a correlation matrix using Pearson's R to visualize trait–trait relationships (Table S13 available as Supplementary Data at *Tree Physiology* Online).

Results

Leaf nitrogen

Increasing soil nitrogen availability increased N_{area} ($P = 0.004$; Table 1; Figure 1a) through marginal increases in N_{mass} ($P = 0.095$; Table 1; Figure 1c) and M_{area} ($P = 0.073$; Table 1; Figure 1e). This pattern appears driven by a positive effect of increasing soil nitrate availability on N_{area} ($P = 0.010$; Table S6 and Figure S3a available as Supplementary Data at *Tree Physiology* Online) through a weak increase in N_{mass} ($P = 0.062$; Table S6 and Figure S3c available as Supplementary Data at *Tree Physiology* Online) and no change in M_{area} ($P = 0.137$; Table S6 and Figure S3e available as Supplementary Data at *Tree Physiology* Online) coupled with a positive effect of increasing soil ammonium availability on N_{area} ($P < 0.002$; Table S6 and Figure S3b available as Supplementary Data at *Tree Physiology* Online) through an increase in M_{area} ($P = 0.007$; Table S6 and Figure S3f available as Supplementary Data at *Tree Physiology* Online) and no change in N_{mass} ($P = 0.977$; Table S6 and Figure S3d available as Supplementary Data at *Tree Physiology* Online).

There was no effect of soil pH on any trait related to leaf nitrogen ($P > 0.1$ in all cases; Table 1; Figure 1b, d, f) when pooled across treatments. However, there was a weak positive effect of increasing soil pH on N_{area} ($P = 0.057$; Table S7 available as Supplementary Data at *Tree Physiology* Online) when models included measurements only from control and sulfur addition plots, a pattern that was driven by a weak positive effect of increasing soil pH on M_{area} ($P = 0.080$; Table S7 available as Supplementary Data at *Tree Physiology* Online) paired with a null effect of soil pH on N_{mass} ($P = 0.240$; Table S7 available as Supplementary Data at *Tree Physiology* Online).

Gas exchange

While there was no effect of soil nitrogen availability on A_{net} ($P = 0.507$; Table 2; Figure 2a) or stomatal conductance ($P = 0.356$; Table 2), increasing soil nitrogen availability had a weak positive effect on V_{cmax25} ($P = 0.063$; Table 2; Figure 2d) and a positive effect on J_{max25} ($P = 0.041$; Table 2; Figure 2g). These effects were primarily associated with changes in soil nitrate availability. Specifically, while soil nitrate availability had no effect on A_{net} ($P = 0.609$; Table S8 and Figure S4a available as Supplementary Data at *Tree Physiology* Online), increasing soil nitrate availability marginally increased V_{cmax25} ($P = 0.052$; Table S8 and Figure S4c available as Supplementary Data at *Tree Physiology* Online) and increased J_{max25} ($P = 0.031$; Table S8 and Figure S4e available as Supplementary Data at *Tree Physiology* Online). There was no effect of increasing soil ammonium availability on A_{net}, V_{cmax25} or J_{max25} ($P > 0.1$ in all cases; Table S8 and Figure S4b, d, f available as Supplementary Data at *Tree Physiology* Online). V_{cmax25} and J_{max25} responses to soil nitrogen availability were similar in magnitude, indicated by a

Table 1. Effects of nitrogen availability and soil pH on *A. saccharum* leaf nitrogen content per unit leaf area (N_{area}), leaf nitrogen content per unit leaf mass (N_{mass}) and leaf mass per unit leaf area (M_{area})*.

		N_{area} ($gN\ m_{leaf}^{-2}$)			N_{mass} ($gN\ g_{leaf}^{-1}$)			M_{area} ($g_{dry\_mass}\ m_{leaf}^{-2}$)		
	df	Coefficient	χ^2	*P*	Coefficient	χ^2	*P*	Coefficient	χ^2	*P*
(Intercept)	–	$4.56*10^{-1}$	–	–	$2.14*10^{0}$	–	–	$1.57*10^{1}$	–	–
Soil N ($\mu g\ N\ g_{resin}^{-1}\ day^{-1}$)	1	$1.84*10^{-2}$	8.388	**0.004**	$1.10*10^{-2}$	2.779	*0.095*	$6.17*10^{-1}$	3.215	*0.073*
Soil pH	1	$1.20*10^{-1}$	0.671	0.413	$4.25*10^{-3}$	0.001	0.978	$6.94*10^{0}$	0.760	0.383

*Significance determined using Type II Wald χ^2 tests ($\alpha = 0.05$). *P*-values less than 0.05 are in bold, while *P*-values between 0.05 and 0.1 are italicized. Model results indicate responses when pooled across all treatments.

Table 2. Effects of nitrogen availability, soil pH and N_{area} on *A. saccharum* leaf gas exchange*.

		A_{net} ($\mu mol\ m^{-2}\ s^{-1}$)			g_s ($mol\ m^{-2}\ s^{-1}$)			V_{cmax25} ($\mu mol\ m^{-2}\ s^{-1}$)		
	df	Coefficient	χ^2	*P*	Coefficient	χ^2	*P*	Coefficient	χ^2	*P*
(Intercept)	–	$3.08*10^{0b}$	–	–	$-2.18*10^{0a}$	–	–	$3.52*10^{1}$	–	–
Soil N ($\mu g\ N\ g_{resin}^{-1}\ day^{-1}$)	1	$-6.64*10^{-3b}$	0.440	0.507	$-1.07*10^{-2a}$	0.853	0.356	$5.95*10^{-1}$	3.441	*0.064*
Soil pH	1	$-2.64*10^{-1b}$	1.291	0.256	$-2.23*10^{-1a}$	0.688	0.407	$-1.11*10^{0}$	0.023	0.879
(N_{area} intercept)	–	$2.16*10^{0b}$	–	–	$-2.66*10^{0a}$	–	–	$1.55*10^{1}$	–	–
N_{area}	1	$-2.62*10^{-1b}$	1.496	0.221	$-5.26*10^{-1a}$	4.861	**0.027**	$1.89*10^{1}$	8.395	**0.004**
		J_{max25} ($\mu mol\ m^{-2}\ s^{-1}$)			J_{max25}:V_{cmax25} (unitless)					
	df	Coefficient	χ^2	*P*	Coefficient	χ^2	*P*			
(Intercept)	–	$7.20*10^{1}$	–	–	$1.57*10^{0}$	–	–			
Soil N ($\mu g\ N\ g_{resin}^{-1}\ day^{-1}$)	1	$1.02*10^{0}$	4.181	**0.041**	$3.91*10^{-3}$	0.405	0.525			
Soil pH	1	$-3.79*10^{0}$	0.111	0.739	$5.57*10^{-2}$	0.152	0.696			
(N_{area} intercept)	–	$4.21*10^{1}$	–	–	$2.11*10^{0}$	–	–			
N_{area}	1	$2.27*10^{1}$	4.435	**0.035**	$-1.97*10^{-1}$	2.278	0.131			

*Significance determined using Type II Wald χ^2 tests ($\alpha = 0.05$). *P*-values less than 0.05 are in bold, while *P*-values between 0.05 and 0.1 are italicized. A superscript 'a' indicates slope coefficients estimated from models fit with natural-log transformed data, while a superscript 'b' indicates coefficients estimated from models fit with square-root transformed data. Relationships between N_{area} and each response variable were fit using a separate mixed-effects model and are independent from results reported for modelled effects of nitrogen and soil pH on each response variable. Model results indicate responses when pooled across all treatments. Key: A_{net}—light saturated net photosynthesis rate; g_s—stomatal conductance; V_{cmax25}—maximum rate of Rubisco carboxylation at 25 °C; J_{max25}—maximum rate of electron transport for RuBP regeneration at 25 °C; J_{max25}:V_{cmax25}—the ratio of J_{max25} to V_{cmax25}.

null effect of increasing soil nitrogen, nitrate and ammonium availability on the ratio of J_{max25} to V_{cmax25} ($P > 0.1$ in all cases; Table 2; Table S8 available as Supplementary Data at *Tree Physiology* Online).

There was no effect of soil pH on any trait related to leaf gas exchange ($P > 0.1$ in all cases; Table 2; Figure 2b, e, h) when pooled across treatments. Null effects of soil pH on A_{net}, stomatal conductance, J_{max25} and J_{max25}:V_{cmax25} persisted when models included only measurements from control and sulfur addition plots ($P > 0.1$ in all cases; Table S9 available as Supplementary Data at *Tree Physiology* Online); however, a weak positive effect of increasing soil pH on V_{cmax25} ($P = 0.054$; Table S9 available as Supplementary Data at *Tree Physiology* Online) emerged.

Despite the lack of relationship between N_{area} and A_{net} ($P = 0.221$; Table 2; Figure 2c), increasing N_{area} was positively associated with V_{cmax25} ($P = 0.004$; Table 2; Figure 2f) and J_{max25} ($P = 0.035$; Table 2; Figure 2i). The null relationship between N_{area} and A_{net} (Figure 2c) likely arose from the strong positive relationship between A_{net} and stomatal conductance ($r^2 = 0.83$) and the negative correlation between N_{area} and stomatal conductance ($r^2 = 0.07$) that was opposite in direction but similar in magnitude to the positive correlation between N_{area} and V_{cmax25} ($r^2 = 0.14$) and positive correlation between N_{area} and J_{max25} ($r^2 = 0.09$) (Table S13 available as Supplementary Data at *Tree Physiology* Online).

Tradeoffs between nitrogen and water use

Analyses that assess the slope relationships between N_{area}, V_{cmax25} and *PNUE* to stomatal conductance across the soil nitrogen and pH gradient are included in Table S11 available as Supplementary Data at *Tree Physiology* Online. These results indicate patterns that are directionally similar but weaker in magnitude than relationships between these traits and χ.

Increasing soil nitrogen availability had a weak negative effect on χ ($P = 0.070$; Table 3; Figure 3a) and *PNUE* ($P = 0.077$; Table 3; Figure 3c). Increasing soil nitrate availability ($P = 0.098$; Table S10 and Figure S5a available as Supplementary Data at *Tree Physiology* Online) and ammonium availability ($P = 0.094$; Table S10 and Figure S5b available as Supplementary Data at *Tree Physiology* Online) each contributed to the negative effect of increasing soil nitrogen availability on χ; however, only soil ammonium availability decreased *PNUE* ($P = 0.031$; Table S10 and Figure S5d available as Supplementary Data at *Tree Physiology* Online). There was also a positive effect of increasing soil

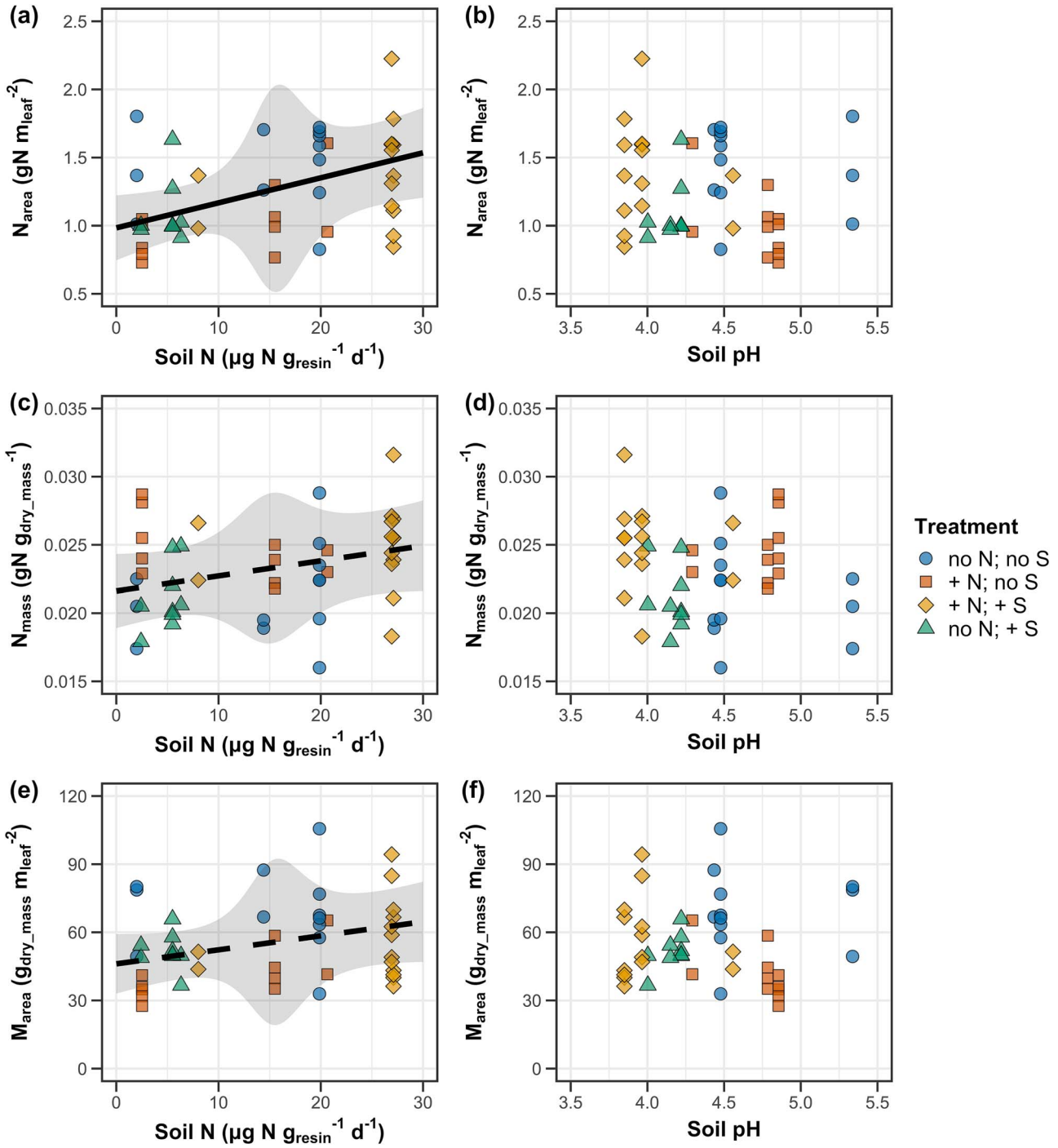

Figure 1. Effects of soil nitrogen availability and soil pH on *A. saccharum* leaf nitrogen content per unit leaf area (a, b), leaf nitrogen content per unit leaf biomass (c, d) and leaf mass per unit leaf area (e, f). Soil nitrogen availability on the x-axis in the left column of panels and soil pH is on the x-axis in the right column of panels. Treatment plots are represented as shaped and colored points. Measurements from the control treatment (no N; no S) are noted with circular points, measurements from the sodium nitrate treatment (+ N; no S) are noted with square points, measurements from the ammonium sulfate treatment (+ N; + S) are noted with diamond points, while measurements from the sulfur treatment (no N; + S) are noted with triangular points. Trendlines that describe the relationship between soil nitrogen availability or soil pH and each response variable are only included when the slope of the regression line is different from zero ($P < 0.05$, solid trendline) or marginally different from zero ($0.05 < P < 0.1$, dashed trendline). Error ribbons indicate the upper and lower 95% confidence interval, drawn across the range in x-axis values using the 'emmeans' R package (Lenth 2019). N = nitrogen, S = sulfur.

nitrogen availability on the N_{area}–χ slope ($P = 0.003$; Table 3; Figure 3e) and the V_{cmax25}–χ slope ($P = 0.036$; Table 3; Figure 3g), but a weak negative effect on the *PNUE*–χ slope ($P = 0.089$; Table 3). Increasing soil nitrate availability and ammonium availability also each contributed to the positive effect of increasing soil nitrogen availability on the N_{area}–χ slope ($P < 0.05$ in both cases; Table S10 and Figure S5e, f available as Supplementary Data at *Tree Physiology* Online); however, the V_{cmax25}–χ slope increased with only increasing soil nitrate availability ($P = 0.033$; Table S10

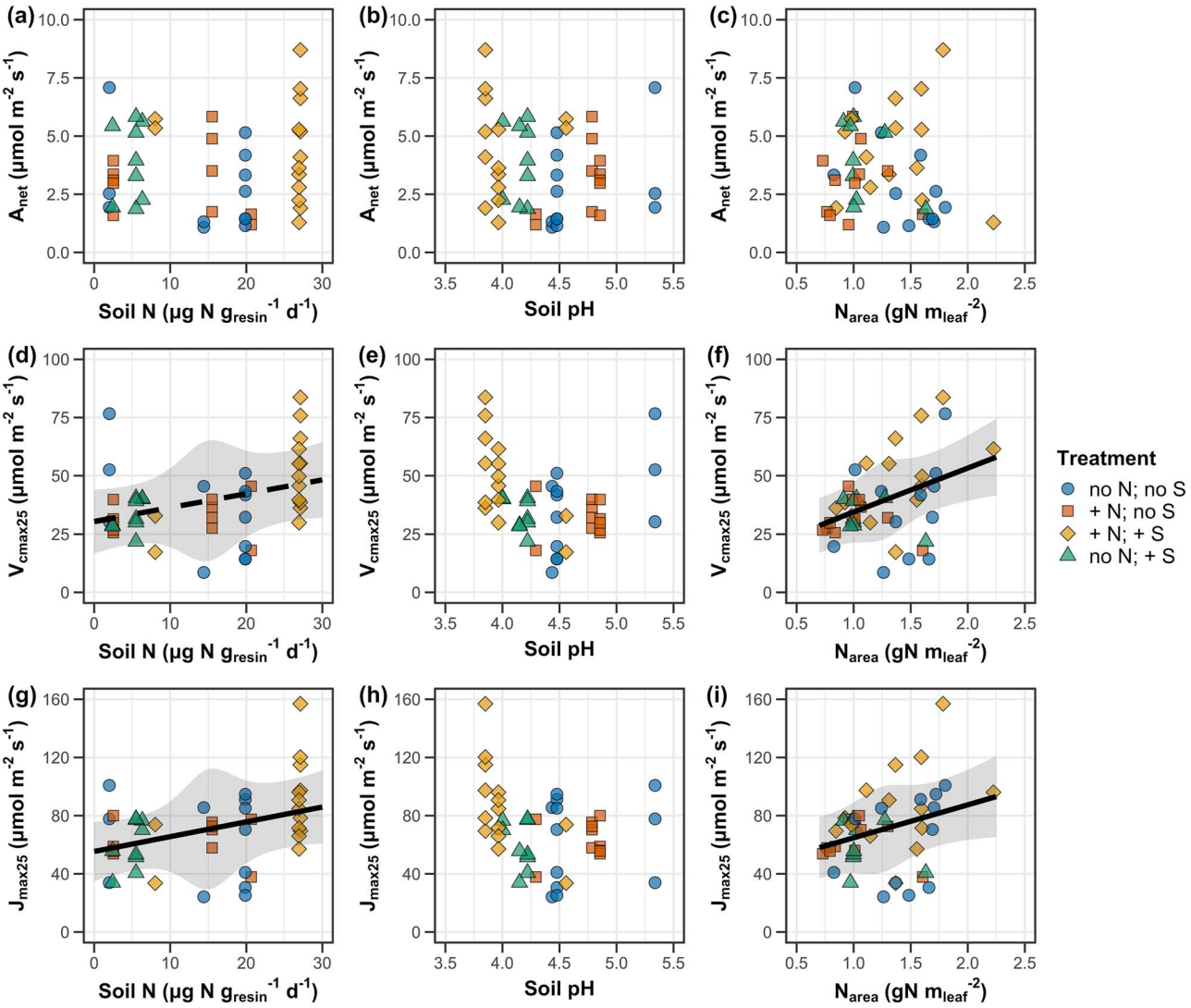

Figure 2. Effects of soil nitrogen availability (left column of panels), soil pH (middle column of panels) and leaf nitrogen content per unit leaf area (right column of panels) on *A. saccharum* net photosynthesis rate per unit leaf area (a–c), maximum Rubisco carboxylation rate per unit leaf area (d–f), and maximum rate of electron transport for RuBP regeneration per unit leaf area (g–i). Soil nitrogen availability is on the x-axis in the left column of panels, soil pH is on the x-axis in the middle column of panels, and leaf nitrogen content per unit leaf area on the x-axis in the right column of panels. Shapes, trendlines and error bars are as explained in Figure 1.

and Figure S5g available as Supplementary Data at *Tree Physiology* Online) and the *PNUE*–χ slope only decreased with increasing soil ammonium availability ($P = 0.068$; Table S10 available as Supplementary Data at *Tree Physiology* Online).

Increasing soil pH had no effect on any trait related to resource-use efficiency ($P > 0.1$ in all cases; Table 3; Figure 3b, d, f, h) when pooled across treatments. When models included only measurements collected from control and sulfur-addition plots, soil pH had no effects on χ, *PNUE* or the *PNUE*–χ slope ($P > 0.1$ in all cases; Table S12 available as Supplementary Data at *Tree Physiology* Online); however, increasing soil pH increased both the N_{area}–χ slope ($P = 0.051$; Table S12 available as Supplementary Data at *Tree Physiology* Online) and the V_{cmax25}–χ slope ($P = 0.031$; Table S12 available as Supplementary Data at *Tree Physiology* Online).

Finally, indices of water-use efficiency showed strong relationships with leaf nitrogen content. The leaf C_i:C_a ratio (χ) decreased steeply with increasing N_{area} ($P < 0.001$; Table 3; Figure 4a), while the V_{cmax25}–χ slope increased with N_{area} ($P < 0.05$; Table 3; Figure 4b). The positive relationship between N_{area} and the V_{cmax25}–χ slope was driven by a positive correlation between N_{area} and V_{cmax25} (Figure 2f) and a negative relationship between N_{area} and χ (Figure 4a). We also found evidence for tradeoffs between nitrogen and water-use efficiency, where χ, an inverse proxy for water-use efficiency, was positively correlated with *PNUE* ($\chi^2 = 14.719$, df = 1, $P < 0.001$; Figure 4c).

Discussion

Photosynthetic least-cost theory provides an explanation for understanding the relationships between nutrient availability, leaf nutrient allocation and photosynthetic capacity. In a given environment, the theory predicts that an increase in soil nutrient availability should allow similar photosynthesis rates to be achieved with increased leaf nutrient content and apparent photosynthetic capacity (i.e. V_{cmax} and J_{max}) at lower leaf C_i:C_a (χ), resulting in an increase in

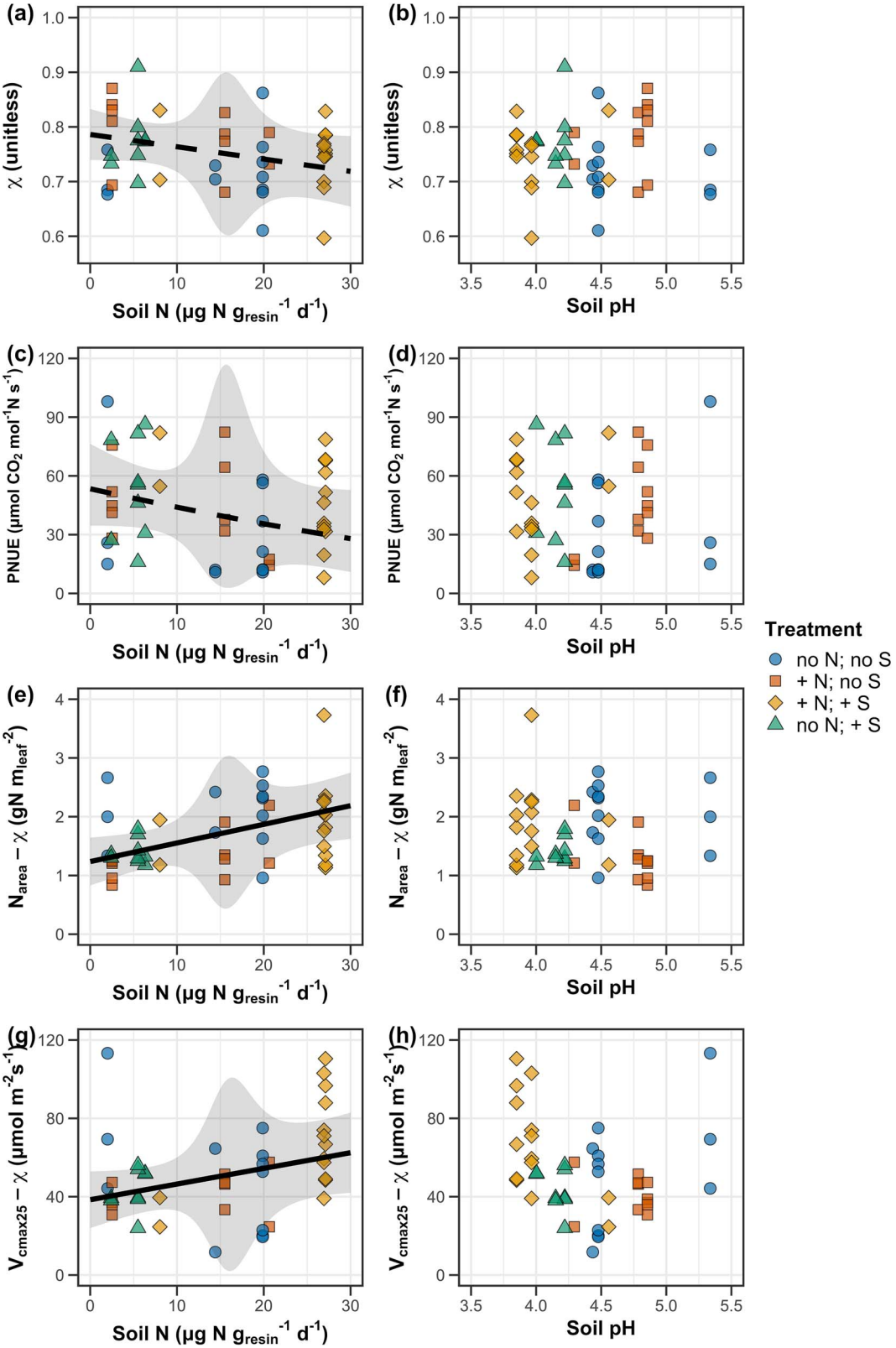

Figure 3. Effects of soil nitrogen availability and soil pH on *A. saccharum* χ (a, b), photosynthetic nitrogen-use efficiency (c, d), the slope relationship between area-based leaf nitrogen content and χ (e, f), and the slope relationship between the maximum Rubisco carboxylation rate and χ (g, h). Soil nitrogen availability on the x-axis in the left column of panels and soil pH is on the x-axis in the right column of panels. Shapes, trendlines and error bars are as explained in Figure 1.

Table 3. Effect of nitrogen availability, soil pH and N_{area} on tradeoffs between nitrogen and water use*.

		χ (unitless)			*PNUE* (μmol CO_2 $mol^{-1}N$ s^{-1})			N_{area}–χ (gN m^{-2})		
	df	Coefficient	χ^2	*P*	Coefficient	χ^2	*P*	Coefficient	χ^2	*P*
(Intercept)	–	$9.31*10^{-1}$	–	–	$1.20*10^{0}$[a]	–	–	$3.39*10^{-3}$	–	–
Soil N (μg N g_{resin}^{-1} day^{-1})	1	$-2.25*10^{-3}$	3.272	*0.070*	$-6.74*10^{-2}$[a]	3.136	*0.077*	$3.17*10^{-2}$	8.557	**0.003**
Soil pH	1	$-3.30*10^{-2}$	1.312	0.252	$-1.07*10^{0}$[a]	1.463	0.227	$2.81*10^{-1}$	1.251	0.263
(N_{area} intercept)	–	$9.02*10^{-1}$	–	–	–	–	–	–	–	–
N_{area}	1	$-1.22*10^{-1}$	43.831	**<0.001**	–	–	–	–	–	–

		V_{cmax25}–χ (μmol m^{-2} s^{-1})			*PNUE*–χ (μmol CO_2 $mol^{-1}N$ s^{-1})		
	df	Coefficient	χ^2	*P*	Coefficient	χ^2	*P*
(Intercept)	–	$8.22*10^{1}$	–	–	$1.40*10^{2}$	–	–
Soil N (μg N g_{resin}^{-1} day^{-1})	1	$8.01*10^{-1}$	4.393	**0.036**	$-1.03*10^{0}$	2.897	*0.089*
Soil pH	1	$-1.00*10^{1}$	1.176	0.278	$1.55*10^{1}$	1.203	0.273
(N_{area} intercept)	–	$4.85*10^{0}$	–	–	–	–	–
N_{area}	1	$1.69*10^{0}$	7.131	**0.008**	–	–	–

*Significance determined using Type II Wald χ^2 tests ($\alpha = 0.05$). *P*-values less than 0.05 are in bold and *P*-values between 0.05 and 0.1 are italicized. A superscript 'a' indicates slope coefficients estimated from linear mixed-effects models fit with square root transformed data. Relationships between N_{area} and each response variable were fit using a separate mixed-effects model and are independent from results reported for relationships between nitrogen and soil pH for each response variable. Model results indicate responses when pooled across all treatments. Key: χ—isotope-derived estimate of the leaf C_i:C_a; *PNUE*—photosynthetic nitrogen-use efficiency, ratio of net photosynthesis to leaf nitrogen content per unit leaf area; N_{area}–χ—slope relationship between N_{area} and χ; V_{cmax25}–χ—slope relationship between V_{cmax25} and χ; *PNUE*–χ—slope relationship between photosynthetic nitrogen-use efficiency and χ.

water-use efficiency, decrease in nutrient-use efficiency, and increase in the slope relationship between leaf nutrient content and χ and the slope relationship between apparent photosynthetic capacity and χ. The theory predicts similar leaf responses to increasing soil pH under acidic conditions, presumably due to generally faster nutrient cycling and lower costs of acquiring nutrients relative to water with increasing soil pH in low pH soils (Wang et al. 2017, Dong et al. 2020, Paillassa et al. 2020).

Here, we take advantage of a nitrogen-by-pH field manipulation experiment to assess whether variability in soil nitrogen availability and soil pH induce nitrogen–water use tradeoffs expected from photosynthetic least-cost theory. Supporting photosynthetic least-cost theory, our results show that as soil nitrogen availability increased, *A. saccharum* net photosynthesis did not change (Figure 2a), even as area-based leaf nitrogen content (Figure 1a) and apparent photosynthetic capacity (Figure 2d, g) increased and χ decreased (Figure 3a). In further support of the theory, increasing soil nitrogen availability reduced photosynthetic nitrogen-use efficiency (Figure 3c), increased the slope relationship between area-based leaf nitrogen content and χ (Figure 3e), increased the slope relationship between apparent photosynthetic capacity and χ (Figure 3g), and decreased the slope relationship between *PNUE* and χ (Table 3). These results indicate that *A. saccharum* individuals maintained net photosynthesis rates in response to increasing soil nitrogen availability by sacrificing inefficient use of a relatively more abundant resource (nitrogen) for more efficient use of a relatively less abundant resource (water). However, there was no effect of soil pH on measured traits, contrasting with our expectations. These findings provide some of the first support for patterns expected from photosynthetic least-cost theory in a field nutrient manipulation experiment and can be used to better understand mechanisms driving leaf nitrogen-photosynthesis relationships across resource availability gradients. Additionally, they can be used to better understand the consequences of atmospheric deposition on plant ecophysiological traits, as these results suggest that nitrogen deposition has a stronger impact on plant communities than soil acidification.

Nitrogen availability modifies tradeoffs between nitrogen and water use

Photosynthetic least-cost theory suggests that reductions in *PNUE* should be driven by an increase in the proportion of leaf nitrogen allocated to photosynthetic enzymes such as Rubisco, a pattern that allows plants to achieve optimal photosynthetic rates with greater photosynthetic capacity to make more efficient use of available light. Following this prediction, increasing soil nitrogen availability increased N_{area} (Figure 1a), V_{cmax25} (Figure 2d) and J_{max25} (Figure 2g) despite no effect of soil nitrogen availability on net photosynthesis (Figure 2a) or stomatal conductance (Table 2). These patterns corresponded with reduced χ with increasing soil nitrogen availability (Figure 3a), and yielding strong positive effects of increasing soil nitrogen availability on the slope relationship between area-based leaf nitrogen content and χ (Figure 3e), and the slope relationship between apparent photosynthetic capacity and χ (Figure 3g), and a negative effect of increasing soil nitrogen availability on the slope relationship between *PNUE* and χ (Table 3). These patterns support nitrogen–water use tradeoffs predicted from the theory.

Positive effects of soil nitrogen availability on area-based leaf nitrogen content (Figure 1a) and apparent photosynthetic capacity (Figure 2d, g) were coupled with a strong positive correlation between area-based leaf nitrogen content and apparent photosynthetic capacity (Table S13 available as Supplementary Data at *Tree Physiology* Online and Figure 2f, i). These results support the idea that *A. saccharum* individuals were using additional nitrogen acquired through increased soil nitrogen availability to enhance photosynthetic

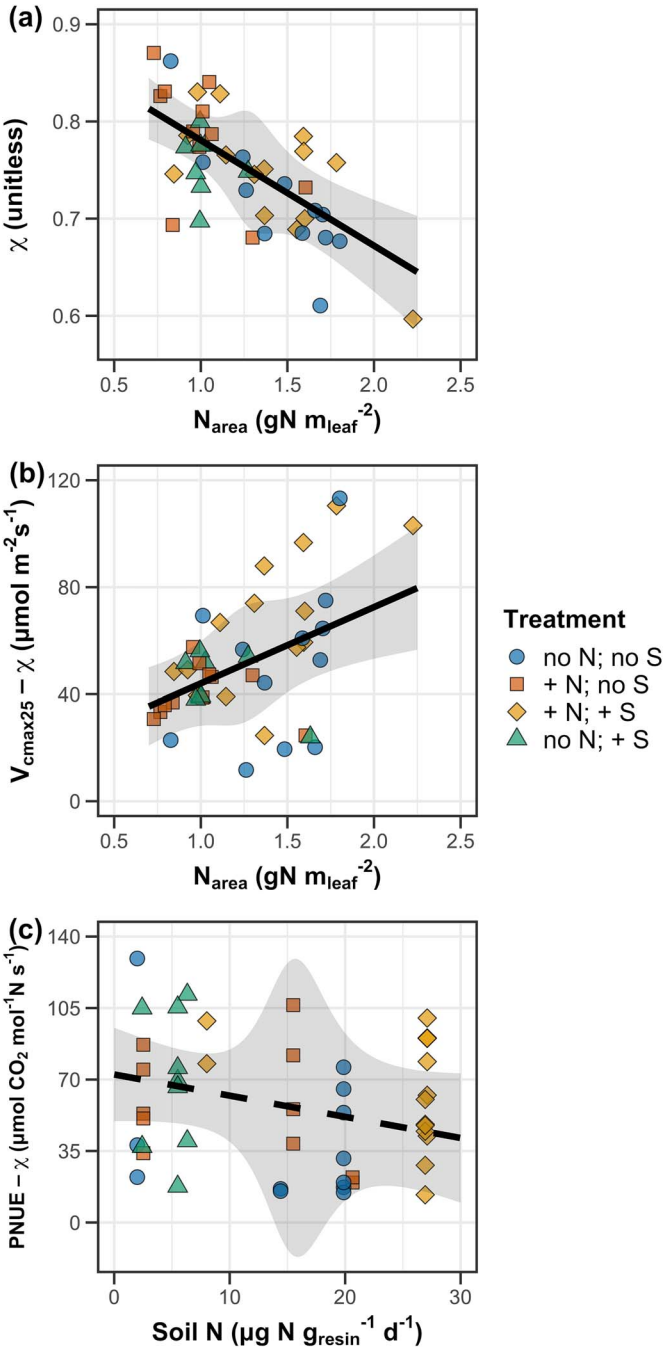

Figure 4. Relationships between *A. saccharum* leaf nitrogen content per unit leaf area and χ (a), leaf nitrogen content per unit leaf area and the maximum Rubisco carboxylation rate per unit χ (b), and χ and photosynthetic nitrogen-use efficiency (c). Leaf nitrogen content per unit leaf area is on the x-axis in panels (a) and (b), while χ is on the x-axis in panel (c). Shapes, trendlines and error bars are as explained in Figure 1.

capacity through increased nitrogen allocation to photosynthetic enzymes (Niinemets and Tenhunen 1997, Wright et al. 2003). However, the stronger response of leaf nitrogen than photosynthetic capacity to soil nitrogen availability (as observed in Waring et al. 2023) suggests that additional nitrogen acquisition due to increased nitrogen availability was also being used to support non-photosynthetic nitrogen pools, possibly to leaf structural tissue or stress-induced amino acid and polyamine synthesis (Minocha et al. 2000, 2019, Onoda et al. 2004, Bubier et al. 2011, Young et al. 2023). Future work should consider explicitly measuring nitrogen allocation to cell wall tissue and stress-induced amino acid synthesis to confirm these hypotheses.

Consistent with the nitrogen–water use tradeoffs predicted from photosynthetic least-cost theory, χ decreased with increasing soil nitrogen availability (Figure 3a) and decreased steeply with increasing area-based leaf nitrogen content (Figure 4a). Further supporting the theory, χ increased with increasing *PNUE* (Figure 4c), and the slope relationship between *PNUE* and χ decreased with increasing nitrogen availability (Table 3). These findings build on previous work using data collected in arid and semi-arid systems (Paillassa

et al. 2020, Querejeta et al. 2022, Westerband et al. 2023), suggesting that nitrogen–water use tradeoffs expected from photosynthetic least-cost theory are consistently observed across terrestrial ecosystems of varying precipitation regimes. However, as suggested in Paillassa et al. (2020) and Querejeta et al. (2022), negative relationships between soil nitrogen availability and χ may become more pronounced with increasing aridity. This strategy could be especially advantageous if it allows individuals growing in arid or semi-arid regions to maintain carbon assimilation rates with reduced water loss. Future work should attempt to quantify the interactive roles of climate and soil nitrogen availability on leaf nitrogen–water use tradeoffs, which could be done using coordinated and multi-factor field nutrient manipulation experiments across climatic gradients, such as the Nutrient Network (Borer et al. 2014).

Tradeoffs between nitrogen and water use were more strongly related to changes in nitrate availability than ammonium availability

Nitrogen–water use tradeoffs were assessed using a summed pool of soil nitrate and ammonium availabilities collected during the gas exchange measurement period. This approach provided an opportunity to isolate the effect of nitrate and ammonium availability on nitrogen–water use tradeoffs across the soil nitrogen availability gradient. Increasing soil nitrate availability was associated with an increase in area-based leaf nitrogen content (Figure S3a available as Supplementary Data at *Tree Physiology* Online), an increase in apparent photosynthetic capacity (Figure S4c, e available as Supplementary Data at *Tree Physiology* Online) and a decrease in χ (Figure S5a available as Supplementary Data at *Tree Physiology* Online). These patterns increased the slope relationship between area-based leaf nitrogen content and χ (Figure S5e available as Supplementary Data at *Tree Physiology* Online) and the slope relationship between apparent photosynthetic capacity and χ (Figure S5g available as Supplementary Data at *Tree Physiology* Online) as soil nitrate availability increased, supporting theoretical expectations. While increased soil ammonium availability was also associated with increased area-based leaf nitrogen content (Figure S3b available as Supplementary Data at *Tree Physiology* Online) and a weak decrease in both χ (Figure S5b available as Supplementary Data at *Tree Physiology* Online) and *PNUE* (Figure S5d available as Supplementary Data at *Tree Physiology* Online), there was no relationship between soil ammonium availability and apparent photosynthetic capacity (Figure S3d, f available as Supplementary Data at *Tree Physiology* Online). The positive response of area-based leaf nitrogen content to increasing soil ammonium availability may have been the product of increased leaf nitrogen allocation to non-photosynthetic pools, as further evidenced by the positive response of M_{area} and the null response of N_{mass} to increasing soil ammonium availability (Onoda et al. 2004, 2017).

Our results suggest that nitrogen–water use tradeoffs across the soil nitrogen availability gradient were more strongly correlated with soil nitrate than soil ammonium availability. These patterns were observed despite the fact that nitrate assimilation is more metabolically costly than ammonium assimilation, as nitrate must be converted to ammonium through a series of energetically expensive reduction reactions before it can be used by the plant (Tischner 2000, Hirel et al. 2011). We therefore expected that nitrate assimilation would be more costly, leading to weaker nitrogen–water use tradeoffs compared with the less costly ammonium assimilation pathway. However, greater costs of nitrate assimilation may be partly offset by its much greater abundance in high-nitrogen soils, and by the greater mobility of nitrate relative to ammonium (Fraterrigo et al. 2011, Zhou et al. 2021). Quantifying the costs of nitrate and ammonium assimilation, along with the associated uptake rates of each form, would help determine if nitrogen–water use tradeoffs were driven by increased nitrate uptake compared with ammonium uptake. Such work would also help determine whether these patterns were driven by the greater variation in soil nitrate availability (plot mean range: 0.55–21.10 μg NO_3-N g_{resin}^{-1} day^{-1}; Table S4 available as Supplementary Data at *Tree Physiology* Online) than soil ammonium availability (plot mean range: 0.51–6.67 μg NH_4-N g_{resin}^{-1} day^{-1}; Table S4 available as Supplementary Data at *Tree Physiology* Online) across plots, which partly confounds our attempts to distinguish the form of nitrogen availability from its total amount. In addition, recent work indicates that the dominant nitrogen form taken up by plants is partly driven by its relative availability (Aanderud and Bledsoe 2009, Liu et al. 2025).

Soil nitrogen availability matters more for determining tradeoffs between nitrogen and water use than soil pH

Previous correlational studies along environmental gradients have identified soil pH as an important edaphic factor that can modify tradeoffs between nutrient and water use (Smith et al. 2019, Paillassa et al. 2020, Westerband et al. 2023) and the proportion of leaf nitrogen allocated to photosynthesis (Luo et al. 2021). Such studies implied that these patterns may be driven by reduced soil nitrogen availability commonly observed in acidic soils, though no prior studies have experimentally evaluated this hypothesis.

When pooled across all treatments, leaf traits were not significantly correlated with soil pH. The lack of an overarching pH response was expected because both of the experimental nitrogen additions increased nitrogen supply, even as one form (ammonium sulfate) decreased soil pH (Table S5 and Figure S2 available as Supplementary Data at *Tree Physiology* Online). When excluding the nitrogen-amended plots and examining measurements collected from only the sulfur addition and control plots, increasing soil pH had no detectable effect on net photosynthesis or χ, but increased area-based leaf nitrogen content and V_{cmax25} (Tables S7 and S9 available as Supplementary Data at *Tree Physiology* Online). These patterns increased the slope relationship between area-based leaf nitrogen content and χ and the slope relationship between V_{cmax25} and χ with increasing soil pH despite no apparent change in *PNUE* across the soil pH gradient (Table S12 available as Supplementary Data at *Tree Physiology* Online).

Directionally, our results support findings from Paillassa et al. (2020) and other gradient studies that note the positive effects of increasing soil pH on area-based leaf nitrogen content and the apparent maximum rate of Rubisco carboxylation, while not supporting expectations of a negative effect of increasing soil pH on χ (Viet et al. 2013, Cornwell et al. 2018, Luo et al. 2021). The range in soil pH values across plots in this study (3.85–5.34) are within the range of soil pH values reported in previous studies that show patterns supportive of least-cost outcomes, although other studies demonstrate support for the theory using a broader range in soil pH values (e.g. Paillassa et al. 2020 use a soil pH range from 3.5 to

8.5). Regardless, our results indicate that increasing soil pH increased leaf nitrogen allocation to photosynthetic enzymes, providing some evidence for pH-driven nitrogen–water use tradeoffs mediated by pH effects on soil nitrogen availability. These results support the role of soil pH in contributing to nitrogen–water tradeoffs because of how soil pH affects soil nitrogen availability, as the larger dataset shows that soil nitrogen availability, regardless of soil pH, was the overriding driver of nitrogen–water use tradeoffs across the soil nitrogen and pH gradients, while modest pH effects emerged in plots with varying pH and no additional nitrogen input.

It is also possible that these observed pH responses may have been driven by changes in phosphorus availability, as phosphorus availability is emerging as a key regulator of relationships between leaf nitrogen and photosynthesis (Jiang et al. 2020, Ellsworth et al. 2022) and is reduced at low soil pH (Hou et al. 2018, 2020). However, acidity-driven suppression of phosphorus availability should have occurred similarly at acidified plots both with and without nitrogen addition and manifested as an overall pH effect, which we did not see in the general models. While phosphorus availability was not measured here, future work should consider phosphorus availability when assessing nutrient–water use tradeoffs across resource availability and soil pH gradients.

Study limitations and future directions

Soil nitrogen availability explained fairly small amounts of variation for all leaf traits. This result is likely due to spatiotemporal variability in both leaf properties and soil nitrogen availability within plots (Akana et al. 2023). However, variance in leaf nitrogen content and photosynthetic processes may be driven by other factors, such as climate-driven changes in demand to build and maintain photosynthetic enzymes (Smith et al. 2019, Prieto et al. 2023, Cheaib et al. 2025*b*) or species phylogeny (Yan et al. 2023). The decision to use a single species in these analyses allowed us to isolate the role of soil nitrogen availability and soil pH on theoretical expectations while controlling for phylogeny. While similar effects of soil nitrogen availability and pH on leaf traits were observed when analyses included measurements collected from all species, interspecies variation generally explained greater variation in leaf traits than explained by the combined effects of soil nitrogen availability and soil pH (Tables S14–S16 and Figures S6–S8 available as Supplementary Data at *Tree Physiology* Online). Understanding how the magnitude and direction of these patterns vary across plant functional groups is an important next step for testing the generality of nitrogen–water use tradeoffs across resource availability gradients.

Gas exchange measurements were collected during a single growing season after multiple years of nutrient addition. The traits measured in this study are highly plastic and known to respond quickly to changes in environmental stimuli; however, these traits can also be influenced by longer-term changes in nutrient allocation, canopy structure or relationships with soil microbiota (e.g. mycorrhizal fungi). The results presented here therefore represent the culmination of both short- and long-term processes that influence measured leaf traits across the soil nitrogen availability and soil pH gradient, although effects of pH could require more than nine years to emerge. Our sampling approach does not allow us to assess the temporal element that regulates leaf-level photosynthetic responses to soil nitrogen availability or soil pH; however, this is an important component of leaf trait variation that future studies should address.

Our treatments might be expected to drive some divergent trajectories in terms of ecosystem biogeochemical cycling and plant-fungal interactions. Nitrate is highly mobile in soils and prone to leaching (Vitousek and Howarth 1991). In contrast, ammonium tends to be more readily retained on soil cation exchange sites and immobilized by soil microbial communities. However, chronically elevated deposition of ammonium can nitrify quickly, especially when plant and microbial capacity for uptake are exceeded (van Breemen et al. 1984), such that nitrate dominates soil nitrogen availability in both types of nitrogen addition in this study, and to date no differences have emerged in any plant or soil response variable (this study, Frey et al. 2025). Long-term increases in soil nitrogen availability should reduce plant investment in mycorrhizal-mediated nitrogen uptake, and has been shown to induce large decreases in soil respiration in both nitrogen treatments, driven in large part by reduced plant allocation belowground to roots and microbial symbionts (Frey et al. 2025). That said, soil microbial communities and most temperate and boreal tree species tend to preferentially assimilate ammonium over nitrate (Templer and Dawson 2004, Fraterrigo et al. 2011, Mao et al. 2025). The lower energetic cost for assimilation of ammonium should produce greater efficiency in its plant uptake than that of nitrate and correspondingly larger tradeoffs with water-use efficiency, and should be a target of future work.

Implications for photosynthetic least-cost theory in the context of changing deposition

Photosynthetic least cost theory indicates that leaf nitrogen content is the product of both (i) leaf nutrient demand to build and maintain photosynthetic enzymes, which is set by aboveground environmental conditions such as light availability, CO_2, temperature or vapor pressure deficit through optimized changes in χ, and (ii) modifications to χ that result from changes in the cost to acquire and use nutrients to build photosynthetic proteins, which can be modified by nutrient availability (Wright et al. 2003, Prentice et al. 2014, Smith et al. 2019, Paillassa et al. 2020, Westerband et al. 2023). This study allowed us to isolate the importance of soil nitrogen availability and soil pH as drivers of these allocation tradeoffs given the close spatial proximity of plots and the experimental manipulations of these two variables. Our results show patterns consistent with those expected from least-cost theory in response to increasing soil nitrogen availability, and weaker patterns in response to increasing soil pH that were primarily driven by increased leaf nitrogen allocation to photosynthetic enzymes.

Our findings—that increasing soil nitrogen availability maintained net photosynthesis rates at reduced nitrogen-use efficiency and increased water-use efficiency—have at least two important implications for interpreting the consequences of changing atmospheric nitrogen deposition. First, Earth system models that do not incorporate frameworks for patterns expected from photosynthetic least-cost theory will likely overestimate the enhancement of photosynthesis by elevated nitrogen deposition and corresponding decreases in evapotranspiration. This overestimation may be particularly apparent if constant nutrient and water-use efficiencies are assumed to be constant across soil nitrogen availability

gradients. Second, concerns for forest productivity are emerging over evidence of increasing nitrogen oligotrophication in the northeastern USA and similar regions where rising atmospheric CO_2 and longer growing seasons combine with reductions in historically elevated nitrogen deposition to increase plant nitrogen limitation (Groffman et al. 2018, Mason et al. 2022). If our results hold for sugar maple and other major forest species in the region, gradual reductions in soil nitrogen availability from these oligotrophication processes could be partly compensated by increased plant nitrogen-use efficiency and reduced water-use efficiency, for lessened impacts on photosynthesis accompanied by increased transpirational water losses.

Conclusions

We used a long-term nitrogen-by-pH experiment to test nitrogen–water use tradeoffs predicted by photosynthetic least-cost theory using the experiment's dominant tree species, *A. saccharum*. Across plots, increasing soil nitrogen availability decreased the ratio of intercellular CO_2 to atmospheric CO_2 (χ, proxy for stomatal conductance and inverse proxy for water-use efficiency), while area-based leaf nitrogen content and apparent photosynthetic capacity increased. However, soil nitrogen availability did not detectably affect net photosynthesis. As a result, photosynthetic nitrogen-use efficiency decreased, and indices of leaf nitrogen content and photosynthetic capacity increased relative to water-use efficiency, as indicated by steeper slope relationships with χ. The decrease in χ with increasing area-based leaf nitrogen content and positive correlation between χ and photosynthetic nitrogen-use efficiency also supported expectations of leaf nitrogen-water tradeoffs.

Altogether, these results provide robust mechanistic support for patterns expected from photosynthetic least-cost theory, among the first to do so in a nutrient manipulation experiment. Our findings also highlight the role of nitrogen–water use tradeoffs as a potential buffering mechanism that enables plants to maintain net photosynthesis rates across gradients of soil resource availability (e.g. due to elevated nitrogen deposition or processes that contribute to nitrogen oligotrophication) by adjusting water- and nitrogen-use efficiencies. Finally, this study provides experimental support for prior work suggesting that leaf nitrogen–water use economies vary with soil nitrogen availability and soil pH, showing that soil nitrogen availability was more important in shaping leaf photosynthetic trait variation than soil pH. These patterns suggest that nitrogen deposition may have a greater influence on plant ecophysiological responses to atmospheric inputs than soil acidification.

Acknowledgments

This research was funded by United States Department of Agriculture NIFA Awards 2015-67003-23485, 2014-67019-21553, and USDA-Hatch NYC-1837402 to C.L.G., E.A.P. and N.G.S. acknowledge support from the National Science Foundation (N.G.S.: DEB-2045968; E.A.P. and N.G.S.: DEB-2217353) and Texas Tech University. E.A.P. and N.G.S. also acknowledge support from the LEMONTREE (Land Ecosystem Models based On New Theory, obseRvations, and ExperimEnts) project, receiving support through Schmidt Sciences, L.L.C. E.A.P. thanks members of the spring 2021 manuscript publishing class at Texas Tech University taught by Tigga Kingston, Brad Posch, and members of the Schwilk and van Gestel lab groups at Texas Tech University for manuscript feedback. Particular thanks go to Risa McNellis (Texas Tech University) and Omair Irfan (Cornell University) for field work assistance and to John Zak at Texas Tech University for supplying reagents needed to process resin bag extracts under global supply chain shortages.

Supplementary Data

Supplementary data for this article are available at *Tree Physiology* Online.

Author contributions

E.A.P. conceptualized the study objectives, conducted field work, completed data analysis and wrote the first manuscript draft. D.W.F. conducted field work, completed laboratory analyses and provided manuscript feedback. C.L.G. designed and has maintained the nutrient addition experiment since its inception, assisted with field work and provided manuscript feedback. N.G.S. conceptualized the study objectives with E.A.P., oversaw data analyses and provided manuscript feedback. All authors approve the manuscript in its current form to be submitted to *Tree Physiology*.

Conflict of interest

None.

Funding

United States Department of Agriculture NIFA Awards 2015-67003-23485, 2014-67019-21553 and USDA-Hatch NYC-1837402; National Science Foundation Awards DEB-2045968 and DEB-2217353; LEMONTREE (Land Ecosystem Models based On New Theory, Observations, and Experiments) project, receiving support through Schmidt Sciences, LLC.

Data availability

All R scripts, data and metadata are available at https://doi.org/10.5281/zenodo.8299010

References

Aanderud ZT, Bledsoe CS (2009) Preferences for ^{15}N-ammonium, ^{15}N-nitrate, and ^{15}N-glycine differ among dominant exotic and subordinate native grasses from a California oak woodland. Environ Exp Bot 65:205–209. https://doi.org/10.1016/j.envexpbot.2008.10.003.

Akana PR, Mifsud IEJ, Menge DNL (2023) Soil nitrogen availability in a temperate forest exhibits large variability at sub-tree spatial scales. Biogeochemistry 164:537–553. https://doi.org/10.1007/s10533-023-01056-5.

Allison SD, Czimczik CI, Treseder KK (2008) Microbial activity and soil respiration under nitrogen addition in Alaskan boreal forest. Glob Chang Biol 14:1156–1168. https://doi.org/10.1111/j.1365-2486.2008.01549.x.

Arnone JA (1997) Indices of plant N availability in an alpine grassland under elevated atmospheric CO_2. Plant Soil 190:61–66. https://doi.org/10.1023/A:1004291618137.

Bae K, Fahey TJ, Yanai RD, Fisk M (2015) Soil nitrogen availability affects belowground carbon allocation and soil respiration in northern hardwood forests of New Hampshire. Ecosystems 18:1179–1191. https://doi.org/10.1007/s10021-015-9892-7.

Bahar NHA, Ishida FY, Weerasinghe LK et al. (2017) Leaf-level photosynthetic capacity in lowland Amazonian and high-elevation Andean tropical moist forests of Peru. New Phytol 214:1002–1018. https://doi.org/10.1111/nph.14079.

Bates D, Mächler M, Bolker B, Walker S (2015) Fitting linear mixed-effects models using lme4. J Stat Softw 67:1–48. https://doi.org/10.18637/jss.v067.i01.

Bernacchi CJ, Singsaas EL, Pimentel C, Portis AR, Long SP (2001) Improved temperature response functions for models of rubisco-limited photosynthesis. Plant Cell Environ 24:253–259. https://doi.org/10.1111/j.1365-3040.2001.00668.x.

Bialic-Murphy L, Smith NG, Voothuluru P, McElderry RM, Roche MD, Cassidy ST, Kivlin SN, Kalisz S (2021) Invasion-induced root–fungal disruptions alter plant water and nitrogen economies. Ecol Lett 24:1145–1156. https://doi.org/10.1111/ele.13724.

Bonan GB, Lawrence PJ, Oleson KW, Levis S, Jung M, Reichstein M, Lawrence DM, Swenson SC (2011) Improving canopy processes in the community land model version 4 (CLM4) using global flux fields empirically inferred from FLUXNET data. J Geophys Res 116:G02014. https://doi.org/10.1029/2010JG001593.

Booth BBB, Jones CD, Collins M et al. (2012) High sensitivity of future global warming to land carbon cycle processes. Environ Res Lett 7:024002. https://doi.org/10.1088/1748-9326/7/2/024002.

Borer ET, Harpole WS, Adler PB, Lind EM, Orrock JL, Seabloom EW, Smith MD (2014) Finding generality in ecology: a model for globally distributed experiments. Methods Ecol Evol 5:65–73. https://doi.org/10.1111/2041-210X.12125.

van Breemen N, Driscoll CT, Mulder J (1984) Acidic deposition and internal proton sources in acidification of soils and waters. Nature 307:599–604. https://doi.org/10.1038/307599a0.

Brix H (1971) Effects of nitrogen fertilization on photosynthesis and respiration in Douglas-fir. For Sci 17:407–414.

Bubier JL, Smith R, Juutinen S, Moore TR, Minocha R, Long S, Minocha S (2011) Effects of nutrient addition on leaf chemistry, morphology, and photosynthetic capacity of three bog shrubs. Oecologia 167:355–368. https://doi.org/10.1007/s00442-011-1998-9.

CASTNET (2024) U.S. Environmental Protection Agency clean air markets division, clean air status and trends network (CASTNET), www.epa.gov/castnet (14 September 2025, date last accessed).

Cheaib A, Chieppa J, Perkowski EA, Smith NG (2025*a*) Soil resource acquisition strategy modulates global plant nutrient and water economics. New Phytol 246:1536–1553. https://doi.org/10.1111/nph.70087.

Cheaib A, Waring EF, McNellis R et al. (2025*b*) Soil nitrogen supply exerts largest influence on leaf nitrogen in environments with the greatest leaf nitrogen demand. Ecol Lett 28:1–13. https://doi.org/10.1111/ele.70015.

Cornwell WK, Wright IJ, Turner J et al. (2018) Climate and soils together regulate photosynthetic carbon isotope discrimination within C_3 plants worldwide. Glob Ecol Biogeogr 27:1056–1067. https://doi.org/10.1111/geb.12764.

Davies-Barnard T, Meyerholt J, Zaehle S et al. (2020) Nitrogen cycling in CMIP6 land surface models: progress and limitations. Biogeosciences 17:5129–5148. https://doi.org/10.5194/bg-17-5129-2020.

Dise NB, Wright RF (1995) Nitrogen leaching from European forests in relation to nitrogen deposition. For Ecol Manage 71:153–161. https://doi.org/10.1016/0378-1127(94)06092-W.

Doane TA, Horwáth WR (2003) Spectrophotometric determination of nitrate with a single reagent. Anal Lett 36:2713–2722. https://doi.org/10.1081/AL-120024647.

Dong N, Prentice IC, Evans BJ, Caddy-Retalic S, Lowe AJ, Wright IJ (2017) Leaf nitrogen from first principles: field evidence for adaptive variation with climate. Biogeosciences 14:481–495. https://doi.org/10.5194/bg-14-481-2017.

Dong N, Prentice IC, Wright IJ et al. (2020) Components of leaf-trait variation along environmental gradients. New Phytol 228:82–94. https://doi.org/10.1111/nph.16558.

Dong N, Prentice IC, Wright IJ et al. (2022) Leaf nitrogen from the perspective of optimal plant function. J Ecol 110:2585–2602. https://doi.org/10.1111/1365-2745.13967.

Driscoll C, Milford JB, Henze DK, Bell MD (2024) Atmospheric reduced nitrogen: sources, transformations, effects, and management. J Air Waste Manage Assoc 74:362–415. https://doi.org/10.1080/10962247.2024.2342765.

Duursma RA (2015) Plantecophys - an R package for analysing and modelling leaf gas exchange data. PloS One 10:e0143346. https://doi.org/10.1371/journal.pone.0143346.

Eastman BA, Adams MB, Brzostek ER, Burnham MB, Carrara JE, Kelly C, McNeil BE, Walter CA, Peterjohn WT (2021) Altered plant carbon partitioning enhanced forest ecosystem carbon storage after 25 years of nitrogen additions. New Phytol 230:1435–1448. https://doi.org/10.1111/nph.17256.

Ellsworth DS, Crous KY, De Kauwe MG et al. (2022) Convergence in phosphorus constraints to photosynthesis in forests around the world. Nat Commun 13:5005. https://doi.org/10.1038/s41467-022-32545-0.

Evans JR (1989) Photosynthesis and nitrogen relationships in leaves of C_3 plants. Oecologia 78:9–19. https://doi.org/10.1007/BF00377192.

Evans JR (2021) Mesophyll conductance: walls, membranes and spatial complexity. New Phytol 229:1864–1876. https://doi.org/10.1111/nph.16968.

Evans JR, Poorter H (2001) Photosynthetic acclimation of plants to growth irradiance: the relative importance of specific leaf area and nitrogen partitioning in maximizing carbon gain. Plant Cell Environ 24:755–767. https://doi.org/10.1046/j.1365-3040.2001.00724.x.

Fan B, Westerband AC, Wright IJ, Gao P, Ding N, Ai D, Tian T, Zhao X, Sun K (2023) Shifts in plant resource use strategies across climate and soil gradients in dryland steppe communities. Plant Soil 497:277–296. https://doi.org/10.1007/s11104-023-06401-z.

Farquhar GD, von Caemmerer S, Berry JA (1980) A biochemical model of photosynthetic CO2 assimilation in leaves of C3 species. Planta 149:78–90. https://doi.org/10.1007/BF00386231.

Farquhar GD, Ehleringer JR, Hubick KT (1989) Carbon isotope discrimination and photosynthesis. Annu Rev Plant Physiol Plant Mol Biol 40:503–537. https://doi.org/10.1146/annurev.pp.40.060189.002443.

Fay PA, Prober SM, Harpole WS et al. (2015) Grassland productivity limited by multiple nutrients. Nat Plants 1:15080. https://doi.org/10.1038/nplants.2015.80.

Firn J, McGree JM, Harvey E et al. (2019) Leaf nutrients, not specific leaf area, are consistent indicators of elevated nutrient inputs. Nat Ecol Evol 3:400–406. https://doi.org/10.1038/s41559-018-0790-1.

Fox J, Weisberg S (2019) An R companion to applied regression, 3rd edn. Sage, Thousand Oaks, CA.

Fraterrigo JM, Strickland MS, Keiser AD, Bradford MA (2011) Nitrogen uptake and preference in a forest understory following invasion by an exotic grass. Oecologia 167:781–791. https://doi.org/10.1007/s00442-011-2030-0.

Frey DW, Kebede E, Sparks JP, Fahey TJ, Goodale CL (2025) Increased soil nitrogen availability suppresses annual soil respiration in mixed temperate forests regardless of acidification. Glob Chang Biol 31:1–15. https://doi.org/10.1111/gcb.70140.

Friedlingstein P, Meinshausen M, Arora VK, Jones CD, Anav A, Liddicoat SK, Knutti R (2014) Uncertainties in CMIP5 climate projections due to carbon cycle feedbacks. J Clim 27:511–526. https://doi.org/10.1175/JCLI-D-12-00579.1.

Ghimire B, Riley WJ, Koven CD, Kattge J, Rogers A, Reich PB, Wright IJ (2017) A global trait-based approach to estimate leaf nitrogen functional allocation from observations. Ecol Appl 27:1421–1434. https://doi.org/10.1002/eap.1542.

Gregory LM, McClain AM, Kramer DM, Pardo JD, Smith KE, Tessmer OL, Walker BJ, Ziccardi LG, Sharkey TD (2021) The triose phosphate utilization limitation of photosynthetic rate: out of global models but important for leaf models. Plant Cell Environ 44:3223–3226. https://doi.org/10.1111/pce.14153.

Groffman PM, Driscoll CT, Durán J et al. (2018) Nitrogen oligotrophication in northern hardwood forests. Biogeochemistry 141: 523–539. https://doi.org/10.1007/s10533-018-0445-y.

Gulmon SL, Chu CC (1981) The effects of light and nitrogen on photosynthesis, leaf characteristics, and dry matter allocation in the chaparral shrub, *Diplacus aurantiacus*. Oecologia 49:207–212. https://doi.org/10.1007/BF00349189.

Harrison SP, Cramer W, Franklin O et al. (2021) Eco-evolutionary optimality as a means to improve vegetation and land-surface models. New Phytol 231:2125–2141. https://doi.org/10.1111/nph.17558.

Hikosaka K, Shigeno A (2009) The role of rubisco and cell walls in the interspecific variation in photosynthetic capacity. Oecologia 160: 443–451. https://doi.org/10.1007/s00442-009-1315-z.

Hirel B, Tétu T, Lea PJ, Dubois F (2011) Improving nitrogen use efficiency in crops for sustainable agriculture. Sustainability 3: 1452–1485. https://doi.org/10.3390/su3091452.

Hou E, Wen D, Kuang Y, Cong J, Chen C, He X, Heenan M, Lu H, Zhang Y (2018) Soil pH predominantly controls the forms of organic phosphorus in topsoils under natural broadleaved forests along a 2500 km latitudinal gradient. Geoderma 315:65–74. https://doi.org/10.1016/j.geoderma.2017.11.041.

Hou E, Luo Y, Kuang Y, Chen C, Lu X, Jiang L, Luo X, Wen D (2020) Global meta-analysis shows pervasive phosphorus limitation of aboveground plant production in natural terrestrial ecosystems. Nat Commun 11:637. https://doi.org/10.1038/s41467-020-14492-w.

IPCC (2021) In: Contribution of Working Group I to the Sixth Assessment Report of the Intergovernmental Panel on Climate Change. Masson-Delmotte V, Zhai P, Pirani A et al. (eds) Climate change 2021: The physical science basis. Cambridge University Press, Cambridge, UK and New York, USA.

Jiang M, Caldararu S, Zhang H et al. (2020) Low phosphorus supply constrains plant responses to elevated CO_2: a meta-analysis. Glob Chang Biol 26:5856–5873. https://doi.org/10.1111/gcb.15277.

Katabuchi M (2015) LeafArea: an R package for rapid digital analysis of leaf area. Ecol Res 30:1073–1077. https://doi.org/10.1007/s11284-015-1307-x.

Kattge J, Knorr W (2007) Temperature acclimation in a biochemical model of photosynthesis: a reanalysis of data from 36 species. Plant Cell Environ 30:1176–1190. https://doi.org/10.1111/j.1365-3040.2007.01690.x.

Kattge J, Knorr W, Raddatz T, Wirth C (2009) Quantifying photosynthetic capacity and its relationship to leaf nitrogen content for global-scale terrestrial biosphere models. Glob Chang Biol 15: 976–991. https://doi.org/10.1111/j.1365-2486.2008.01744.x.

Keeling CD, Mook WG, Tans PP (1979) Recent trends in the $^{13}C/^{12}C$ ratio of atmospheric carbon dioxide. Nature 277:121–123. https://doi.org/10.1038/277121a0.

Kenward MG, Roger JH (1997) Small sample inference for fixed effects from restricted maximum likelihood. Biometrics 53:983. https://doi.org/10.2307/2533558.

Knorr W (2000) Annual and interannual CO_2 exchanges of the terrestrial biosphere: process-based simulations and uncertainties. Glob Ecol Biogeogr 9:225–252. https://doi.org/10.1046/j.1365-2699.2000.00159.x.

Knorr W, Heimann M (2001) Uncertainties in global terrestrial biosphere modeling: 1. A comprehensive sensitivity analysis with a new photosynthesis and energy balance scheme. Global Biogeochem Cycles 15:207–225. https://doi.org/10.1029/1998GB001059.

Kolář T, Čermák P, Oulehle F, Trnka M, Štěpánek P, Cudlín P, Hruška J, Büntgen U, Rybníček M (2015) Pollution control enhanced spruce growth in the "black triangle" near the Czech–Polish border. Sci Total Environ 538:703–711. https://doi.org/10.1016/j.scitotenv.2015.08.105.

LeBauer DS, Treseder K (2008) Nitrogen limitation of net primary productivity in terrestrial ecosystems is globally distributed. Ecology 89:371–379. https://doi.org/10.1890/06-2057.1.

Lenth R (2019) Emmeans: estimated marginal means, aka least-squares means. https://doi.org/10.32614/CRAN.package.emmeans.

Li W, Zhang H, Huang G, Liu R, Wu H, Zhao C, McDowell NG (2020) Effects of nitrogen enrichment on tree carbon allocation: a global synthesis. Glob Ecol Biogeogr 29:573–589. https://doi.org/10.1111/geb.13042.

Li Z, Tian D, Wang B et al. (2019) Microbes drive global soil nitrogen mineralization and availability. Glob Chang Biol 25:1078–1088. https://doi.org/10.1111/gcb.14557.

Liang X, Zhang T, Lu X et al. (2020) Global response patterns of plant photosynthesis to nitrogen addition: a meta-analysis. Glob Chang Biol 26:3585–3600. https://doi.org/10.1111/gcb.15071.

Liu M, Xu X, Wanek W et al. (2025) Nitrogen availability in soil controls uptake of different nitrogen forms by plants. New Phytol 245:1450–1467. https://doi.org/10.1111/nph.20335.

Lovett GM, Mitchell MJ (2004) Sugar maple and nitrogen cycling in the forests of eastern North America. Front Ecol Environ 2:81–88. https://doi.org/10.1890/1540-9295(2004)002[0081:SMANCI]2.0.CO;2.

Luo X, Keenan TF, Chen JM et al. (2021) Global variation in the fraction of leaf nitrogen allocated to photosynthesis. Nat Commun 12:4866. https://doi.org/10.1038/s41467-021-25163-9.

Mao J, Wang J, Liao J, Xu X, Tian D, Zhang R, Peng J, Niu S (2025) Plant nitrogen uptake preference and drivers in natural ecosystems at the global scale. New Phytol 246:972–983. https://doi.org/10.1111/nph.70030.

Mason RE, Craine JM, Lany NK et al. (2022) Evidence, causes, and consequences of declining nitrogen availability in terrestrial ecosystems. Science 376:376. https://doi.org/10.1126/science.abh3767.

Medlyn BE, Dreyer E, Ellsworth DS et al. (2002) Temperature response of parameters of a biochemically based model of photosynthesis. II. A review of experimental data. Plant Cell Environ 25:1167–1179. https://doi.org/10.1046/j.1365-3040.2002.00891.x.

Menne MJ, Durre I, Vose RS, Gleason BE, Houston TG (2012) An overview of the global historical climatology network-daily database. J Atmos Oceanic Tech 29:897–910. https://doi.org/10.1175/JTECH-D-11-00103.1.

Minocha R, Long S, Magill AH, Aber JD, McDowell WH (2000) Foliar free polyamine and inorganic ion content in relation to soil and soil solution chemistry in two fertilized forest stands at the Harvard Forest, Massachusetts. Plant Soil 222-222:119–137. https://doi.org/10.1023/A:1004775829678.

Minocha R, Long S, Turlapati SA, Fernandez I (2019) Dynamic species-specific metabolic changes in the trees exposed to chronic N+S additions at the bear brook watershed in Maine, USA. Ann For Sci 76:25. https://doi.org/10.1007/s13595-019-0808-0.

Niinemets Ü, Tenhunen JD (1997) A model separating leaf structural and physiological effects on carbon gain along light gradients for the shade-tolerant species *Acer saccharum*. Plant Cell Environ 20:845–866. https://doi.org/10.1046/j.1365-3040.1997.d01-133.x.

Onoda Y, Hikosaka K, Hirose T (2004) Allocation of nitrogen to cell walls decreases photosynthetic nitrogen-use efficiency. Funct Ecol 18:419–425. https://doi.org/10.1111/j.0269-8463.2004.00847.x.

Onoda Y, Wright IJ, Evans JR, Hikosaka K, Kitajima K, Niinemets Ü, Poorter H, Tosens T, Westoby M (2017) Physiological and structural tradeoffs underlying the leaf economics spectrum. New Phytol 214: 1447–1463. https://doi.org/10.1111/nph.14496.

Paillassa J, Wright IJ, Prentice IC et al. (2020) When and where soil is important to modify the carbon and water economy of leaves. New Phytol 228:121–135. https://doi.org/10.1111/nph.16702.

Peng Y, Bloomfield KJ, Cernusak LA, Domingues TF, Prentice IC (2021) Global climate and nutrient controls of photosynthetic capacity. Commun Biol 4:462. https://doi.org/10.1038/s42003-021-01985-7.

Perkowski EA, Waring EF, Smith NG (2021) Root mass carbon costs to acquire nitrogen are determined by nitrogen and light availability in two species with different nitrogen acquisition strategies. J Exp Bot 72:5766–5776. https://doi.org/10.1093/jxb/erab253.

Perkowski EA, Ezekannagha E, Smith NG (2025) Nitrogen demand, availability, and acquisition strategy control plant responses to

elevated CO_2. J Exp Bot 76:2908–2923. https://doi.org/10.1093/jxb/eraf118.
Perkowski EA, Terrones J, German HL, Smith NG (2024) Symbiotic nitrogen fixation reduces belowground biomass carbon costs of nitrogen acquisition under low, but not high, nitrogen availability. AoB Plants 16:1–22. https://doi.org/10.1093/aobpla/plae051.
Pons TL, Pearcy RW (1994) Nitrogen reallocation and photosynthetic acclimation in response to partial shading in soybean plants. Physiol Plant 92:636–644. https://doi.org/10.1111/j.1399-3054.1994.tb03034.x.
Prentice IC, Dong N, Gleason SM, Maire V, Wright IJ (2014) Balancing the costs of carbon gain and water transport: testing a new theoretical framework for plant functional ecology. Ecol Lett 17:82–91. https://doi.org/10.1111/ele.12211.
Prentice IC, Liang X, Medlyn BE, Wang Y-P (2015) Reliable, robust and realistic: the three R's of next-generation land-surface modelling. Atmos Chem Phys 15:5987–6005. https://doi.org/10.5194/acp-15-5987-2015.
Prieto I, León-Sánchez L, Nicolás E, Nortes P, Querejeta JI (2023) Warming reduces both photosynthetic nutrient use efficiency and water use efficiency in Mediterranean shrubsWarming reduces nutrient use efficiency. Environ Exp Bot 210:105331. https://doi.org/10.1016/j.envexpbot.2023.105331.
Querejeta JI, Prieto I, Armas C et al. (2022) Higher leaf nitrogen content is linked to tighter stomatal regulation of transpiration and more efficient water use across dryland trees. New Phytol 235:1351–1364. https://doi.org/10.1111/nph.18254.
R Core Team (2021) R: A language and environment for statistical computing. R Foundation for Statistical Computing, Vienna, Austria. https://www.R-project.org/.
Rhine ED, Mulvaney RL, Pratt EJ, Sims GK (1998) Improving the Berthelot reaction for determining ammonium in soil extracts and water. Soil Sci Soc Am J 62:473–480. https://doi.org/10.2136/sssaj1998.03615995006200020026x.
Rogers A (2014) The use and misuse of V c,max in earth system models. Photosynth Res 119:15–29. https://doi.org/10.1007/s11120-013-9818-1.
Rogers A, Medlyn BE, Dukes JS et al. (2017) A roadmap for improving the representation of photosynthesis in earth system models. New Phytol 213:22–42. https://doi.org/10.1111/nph.14283.
Schaefer K, Schwalm CR, Williams C et al. (2012) A model-data comparison of gross primary productivity: results from the north American carbon program site synthesis. J Geophys Res Biogeosci 117:G03010. https://doi.org/10.1029/2012JG001960.
Schneider CA, Rasband WS, Eliceiri KW (2012) NIH image to ImageJ: 25 years of image analysis. Nat Methods 9:671–675. https://doi.org/10.1038/nmeth.2089.
Smith NG, Lombardozzi DL, Tawfik A, Bonan GB, Dukes JS (2017) Biophysical consequences of photosynthetic temperature acclimation for climate. J Adv Model Earth Syst 9:536–547. https://doi.org/10.1002/2016MS000732.
Smith NG, Malyshev SL, Shevliakova E, Kattge J, Dukes JS (2016) Foliar temperature acclimation reduces simulated carbon sensitivity to climate. Nat Clim Chang 6:407–411. https://doi.org/10.1038/nclimate2878.
Smith NG, Dukes JS (2013) Plant respiration and photosynthesis in global-scale models: incorporating acclimation to temperature and CO_2. Glob Chang Biol 19:45–63. https://onlinelibrary.wiley.com/doi/10.1111/j.1365-2486.2012.02797.x.
Smith NG, Dukes JS (2018) Drivers of leaf carbon exchange capacity across biomes at the continental scale. Ecology 99:1610–1620. https://doi.org/10.1002/ecy.2370.
Smith NG, Keenan TF, Prentice IC et al. (2019) Global photosynthetic capacity is optimized to the environment. Ecol Lett 22:506–517. https://doi.org/10.1111/ele.13210.
Soil Survey Staff (2022) Web soil survey. Natural Resources Conservation Service, United States Department of Agriculture. Available from: http://websoilsurvey.sc.egov.usda.gov/ (18 November 2022, date last accessed).
Stocker BD, Dong N, Perkowski EA et al. (2025) Empirical evidence and theoretical understanding of ecosystem carbon and nitrogen cycle interactions. New Phytol 245:49–68. https://doi.org/10.1111/nph.20178.
Templer PH, Dawson TE (2004) Nitrogen uptake by four tree species of the Catskill Mountains, New York: implications for forest N dynamics. Plant Soil 262:251–261.
Tischner R (2000) Nitrate uptake and reduction in higher and lower plants. Plant Cell Environ 23:1005–1024. https://doi.org/10.1046/j.1365-3040.2000.00595.x.
Truog E (1947) Soil reaction influence on availability of plant nutrients. Soil Sci Soc Am J 11:305–308. https://doi.org/10.2136/sssaj1947.036159950011000C0057x.
Vet R, Artz RS, Carou S et al. (2014) A global assessment of precipitation chemistry and deposition of sulfur, nitrogen, sea salt, base cations, organic acids, acidity and pH, and phosphorus. Atmos Environ 93:3–100. https://doi.org/10.1016/j.atmosenv.2013.10.060.
Viet HD, Kwak J-H, Lee K-S, Lim S-S, Matsushima M, Chang SX, Lee K-H, Choi W-J (2013) Foliar chemistry and tree ring $\delta^{13}C$ of *Pinus densiflora* in relation to tree growth along a soil pH gradient. Plant Soil 363:101–112. https://doi.org/10.1007/s11104-012-1301-9.
Vitousek PM, Howarth RW (1991) Nitrogen limitation on land and in the sea: how can it occur? Biogeochemistry 13:87–115. https://doi.org/10.1007/BF00002772.
Walker AP, Beckerman AP, Gu L et al. (2014) The relationship of leaf photosynthetic traits - V_{cmax} and J_{max} - to leaf nitrogen, leaf phosphorus, and specific leaf area: a meta-analysis and modeling study. Ecol Evol 4:3218–3235. https://doi.org/10.1002/ece3.1173.
Wang H, Prentice IC, Keenan TF, Davis TW, Wright IJ, Cornwell WK, Evans BJ, Peng C (2017) Towards a universal model for carbon dioxide uptake by plants. Nat Plants 3:734–741. https://doi.org/10.1038/s41477-017-0006-8.
Waring EF, Perkowski EA, Smith NG (2023) Soil nitrogen fertilization reduces relative leaf nitrogen allocation to photosynthesis. J Exp Bot 74:5166–5180. https://doi.org/10.1093/jxb/erad195.
Weatherburn MW (1967) Phenol-hypochlorite reaction for determination of ammonia. Anal Chem 39:971–974. https://doi.org/10.1021/ac60252a045.
Westerband AC, Wright IJ, Maire V et al. (2023) Coordination of photosynthetic traits across soil and climate gradients. Glob Chang Biol 29:856–873. https://doi.org/10.1111/gcb.16501.
Wieder WR, Grandy AS, Kallenbach CM, Taylor PG, Bonan GB (2015) Representing life in the earth system with soil microbial functional traits in the MIMICS model. Geosci Model Dev 8:1789–1808. https://doi.org/10.5194/gmd-8-1789-2015.
Wieder WR, Lawrence DM, Fisher RA et al. (2019) Beyond static benchmarking: using experimental manipulations to evaluate land model assumptions. Global Biogeochem Cycles 33:1289–1309. https://doi.org/10.1029/2018GB006141.
Wright IJ, Reich PB, Westoby M (2003) Least-cost input mixtures of water and nitrogen for photosynthesis. Am Nat 161:98–111. https://doi.org/10.1086/344920.
Yan Z, Sardans J, Peñuelas J et al. (2023) Global patterns and drivers of leaf photosynthetic capacity: the relative importance of environmental factors and evolutionary history. Glob Ecol Biogeogr 32:668–682. https://doi.org/10.1111/geb.13660.
Young AR, Minocha R, Long S, Drake JE, Yanai RD (2023) Patterns of physical, chemical, and metabolic characteristics of sugar maple leaves with depth in the crown and in response to nitrogen and phosphorus addition. Tree Physiol 43:1118–1129. https://doi.org/10.1093/treephys/tpad043.
Zaehle S, Sitch S, Smith B, Hatterman F (2005) Effects of parameter uncertainties on the modeling of terrestrial biosphere

dynamics. Global Biogeochem Cycles 19:GB3020. https://doi.org/10.1029/2004GB002395.

Zhou K, Xu W, Zhang L, Ma M, Liu X, Zhao Y (2023) Estimating nitrogen and sulfur deposition across China during 2005 to 2020 based on multiple statistical models. Atmos Chem Phys 23:8531–8551. https://doi.org/10.5194/acp-23-8531-2023.

Zhou X, Wang A, Hobbie EA et al. (2021) Mature conifers assimilate nitrate as efficiently as ammonium from soils in four forest plantations. New Phytol 229:3184–3194. https://doi.org/10.1111/nph.17110.

Ziehn T, Kattge J, Knorr W, Scholze M (2011) Improving the predictability of global CO_2 assimilation rates under climate change. Geophys Res Lett 38:L10404.

Tree Physiology, 2025, 45, tpaf119
https://doi.org/10.1093/treephys/tpaf119
Research paper